Palaeomagnetism, geochronology and geochemistry of the Palaeoproterozoic Rabbit Creek and Powder River dyke swarms: implications for Wyoming in supercraton Superia

TAYLOR M. KILIAN[1]*, WOUTER BLEEKER[2], KEVIN CHAMBERLAIN[3], DAVID A. D. EVANS[1] & BRIAN COUSENS[4]

[1]*Department of Geology and Geophysics, Yale University, 210 Whitney Ave, New Haven, CT 06511, USA*

[2]*Geological Survey of Canada, 601 Booth Street, Ottawa, ON, Canada K1A 0E8*

[3]*Department of Geology and Geophysics, University of Wyoming, Laramie, WY 82071-3006, USA*

[4]*Ottawa–Carleton Geoscience Centre, Department of Earth Sciences, Carleton University, 1125 Colonel By Drive, Ottawa, ON, Canada K1S 5B6*

**Corresponding author (e-mail: taylor.kilian1@gmail.com)*

Abstract: It is likely that Archaean cratons of Laurentia had different palaeogeographic histories prior to their amalgamation. New palaeomagnetic, geochronological and geochemical evidence supports a reconstruction of the Wyoming craton adjacent to the southern margin of the Superior craton at 2.16 Ga, before rifting (*c.* 2.1–2.0 Ga) and eventual reamalgamation after the Hudsonian Orogeny (*c.* 1.8 Ga). U–Pb ages (TIMS on baddeleyite) from five dykes yield two groups of ages at *c.* 2164 and 2155 Ma. The younger group of ages defines the Rabbit Creek swarm at 2161–2152 Ma and precisely dates its palaeomagnetic pole. Two large and differentiated dykes (>100 m) in the Bighorn and Wind River uplifts are geographically related to the Rabbit Creek swarm but have slightly different orientations and yield slightly older ages at 2171–2157 Ma. These dykes may be parts of a single intrusion (the 'Great Dyke of Wyoming') that spans over 200 km between uplifts, possibly representing a different magmatic event. This older event does not have enough distinct intrusions to provide a correctly averaged palaeomagnetic pole, but correlates with magmatism in the Superior craton and has a palaeomagnetic remanence comparable to the Rabbit Creek dykes. With minor tilt corrections, the palaeomagnetic data from the Rabbit Creek swarm and Powder River–South Pass dykes support a reconstruction of the southeastern Wyoming craton against the southern Superior craton. This fit juxtaposes the Palaeoproterozoic Huronian and Snowy Pass Supergroups along two passive margins that experienced a prolonged period of mafic magmatism (>100 myr) and rift basin development. Although there are slight geochemical variations across the Rabbit Creek swarm, all dykes fit into two distinct groups that are independently dated and internally consistent.

Supplementary material: Supporting figures and locality tables are available at www.geolsoc.org.uk/SUP18824

The Archaean cratons scattered around the globe often contain collisional belts, ancient rifted margins and multiple generations of dyke swarms, suggestive of horizontal plate motions and continental amalgamations. Supercontinent Nuna was hypothesized by recognizing the worldwide distribution of collisional belts in the 2100–1800 Ma interval (Hoffman 1997; a.k.a. Columbia: Rogers & Santosh 2002; Zhao *et al.* 2002), and depended on a major focus on the Proterozoic history of Laurentia (Hoffman 1988; Ansdell *et al.* 2005; St-Onge *et al.* 2006). These same tectonic markers also suggest that many of these Archaean fragments were connected even earlier (Bleeker 2003; Bleeker & Ernst 2006), but perhaps in different configurations. This study focuses mainly on dyke swarms, the intrusive remnants of large igneous provinces, which are excellent tools for testing Precambrian continental reconstructions (Bleeker & Ernst 2006). Mafic dyke swarms signal possible rifting events and hotspot magmatism while they also contain the ideal mineralogical assemblage for palaeomagnetic and geochronological studies. In addition, when dyke swarms intrude two landmasses in the process

From: Li, Z. X., Evans, D. A. D. & Murphy, J. B. (eds) 2016. *Supercontinent Cycles Through Earth History*. Geological Society, London, Special Publications, **424**, 15–45.
First published online June 4, 2015, http://doi.org/10.1144/SP424.7

of rifting, the orientations of the dykes often converge on a piercing point along the rifted margins (Ernst & Bleeker 2010). The piercing point provides additional insight into possible palaeogeographic correlations and also aids in the refinement of palaeomagnetically derived reconstructions.

The Wyoming craton hosts a large number of dyke swarms that occur in high densities throughout almost every region of exposed Archaean/Proterozoic rock (Snyder *et al.* 1989). Although a handful of magmatic events have been studied, dating from the Neoarchaean Era through the Neoproterozoic Era, it is difficult to establish conclusively whether or not these magmatic events can be correlated across the craton, since the limited and sporadic exposures of Precambrian crust reveal as little as 10% of the whole craton. Precambrian basement exposures resulted largely from differential uplift during the Laramide Orogeny (80–55 Ma), thrusting large basement blocks up and past kilometres of Phanaerozoic sedimentary rocks. This created a handful of windows to view the craton (Love & Christiansen 1985; Fan & Carrapa 2014); hence the Wyoming craton requires several important and somewhat unique questions to be addressed before using mafic dyke swarms to test reconstructions. (1) Is the basement geology of the different Laramide uplifts coherent enough to allow a craton-wide approach? In other words, can we correlate dyke events and palaeomagnetic data between uplifts in detail and correct for minor rotations, or has Laramide tectonics made the problem intractable? (2) Are enough dykes of each swarm exposed to average out secular variation of the Earth's magnetic field and to provide a statistically significant palaeomagnetic pole? After satisfying those concerns, to which Archaean blocks can we compare our data with and which pieces may have been adjacent to Wyoming?

The best approach in solving these questions is to establish precise ages and primary palaeomagnetic poles for regional dyke swarms, correlate these between uplifts, and apply minor inter-uplift structural corrections where necessary, thereby establishing a detailed magmatic barcode and apparent polar wander path for Wyoming craton as a whole prior to its incorporation into Laurentia. In this study we also determined the whole-rock composition of some of the dykes with two aims in mind: to distinguish each swarm geochemically and to identify geochemical trends within swarms.

Herein we present a palaeomagnetic pole for the Rabbit Creek dyke swarm at 2152–2161 Ma, which includes independent age analyses from three different dykes exposed in the Bighorn Mountains. We also compare results with those of Harlan *et al.* (2003), refining the age of the large intrusion in the Wind River Range and connecting it to a very similar intrusion more than 200 km away in the Bighorn Mountains. These two magmatic events probably represent individual pulses of a protracted interval of magmatism along the margin of Wyoming craton (2170–2000 Ma), correlating well with mafic dyke swarms from southern Superior and other cratons worldwide.

Background geology

Wyoming in Laurentia

The Wyoming craton arrived at its current position during the amalgamation of Laurentia at *c.* 1800–1700 Ma (e.g. St-Onge *et al.* 2006). The dating of the sutures surrounding Wyoming suggests multiple episodes of metamorphism, making it more difficult to identify the exact order of collisions and whether any pieces were contiguous with Wyoming prior to collision (Dahl *et al.* 1999; Mueller *et al.* 2002, 2005). Most importantly, all of the available ages for the suture zones surrounding Wyoming are younger than *c.* 1900 Ma, indicating that, before incorporation into Laurentia, Wyoming was either by itself or with other fragments that subsequently rifted away.

Some attempts to recognize prior connections to Wyoming (before *c.* 1800 Ma) have focused on the Snowy Pass Supergroup passive margin sequence in the Medicine Bow Mountains of the SE Wyoming craton (Graff 1979; Bekker & Eriksson 2003). Many scientists have recognized similarities between the Snowy Pass Supergroup and the Huronian Supergroup of the southern Superior craton (Roscoe 1969), especially the distinct glaciogenic strata found in both sections (Blackwelder 1926) and their possible relationships to other glaciogenic sediments in North America (Young 1970; Graff 1979; Houston 1993; Young *et al.* 2001). Some workers have suggested that deposition could have taken place in separate locations on Earth (Karlstrom *et al.* 1983), especially if the glacial episodes were worldwide in nature. Other studies hypothesized that, with Wyoming and Superior in their current configuration, deposition could have taken place along the same, contiguous southern margin of Laurentia (Houston 1993; Aspler & Chiarenzelli 1998). Roscoe & Card (1993) qualitatively defined a reconstruction of southeastern Wyoming against southern Superior, placing palaeocurrent data from both sequences into agreement with stratigraphic correlations. The intrusion of the Nipissing diabase sills at *c.* 2215 Ma into the Huronian Supergroup (Noble & Lightfoot 1992) constrains the age of the reconstructions, which may correlate with metamorphosed intrusions within the Snowy Pass Supergroup in Wyoming. Our newly recognized Wyoming events postdate the Nipissing magmatic event and are probably related to subsequent circum-Superior rifting, possibly from the creation of another nearby rift basin or from distal, continental-scale stresses. Multiple dyke swarms within the Superior craton record similar stresses and magmatism during this broad time interval, providing many possible correlative events along Superior's southern margin.

Geology of Wyoming

The Archaean framework of the Wyoming craton or province can be divided into four tectonic subprovinces (Fig. 1): (1) the Montana metasedimentary terrane (MMT); (2) the Bighorn subprovince; (3) the Sweetwater subprovince; and (4) the southern accreted terranes (SAT) (Chamberlain *et al.* 2003; Frost *et al.* 2006*b*; Mueller & Frost 2006; Chamberlain & Mueller 2007). The core of the craton is dominated by the 2900–2800 Ma plutons in the Bighorn and Sweetwater subprovinces, including high-Na tonalite–trondhjemite–granodiorite and high-K, calc–alkaline magmatism (Frost *et al.* 1998, 2006*a*; Chamberlain *et al.* 2003; Frost & Fanning 2006). A handful of plutonic and supracrustal ages greater than 3000 Ma also exist (Mueller *et al.* 1996; Grace *et al.* 2006; Chamberlain & Mueller 2007). The MMT is a smaller terrane on the NW margin of Wyoming that contains some of the oldest exposed rocks in the craton (Mogk *et al.* 1992). Meta-supracrustal rocks dominate the MMT, in contrast to the rest of the Wyoming province. However, the enriched $^{207}Pb/^{204}Pb$ isotopic signatures measured in rocks throughout the MMT, Bighorn and Sweetwater subprovinces are fairly unique in Archaean cratons and suggest the same source region of crustal extraction (Mueller & Frost 2006). The simplest interpretation is that all three subprovinces grew as part of a single larger continental province, yet they experienced different histories until their unification in the Neoarchaean Era at *c.* 2.7 Ga (Mogk *et al.* 1988, 1992). Other Archaean cratons that show the same enriched isotopic signature include the North Atlantic, Slave, Zimbabwe and Yilgarn cratons (Luais & Hawkesworth 2002; Kamber *et al.* 2003).

In contrast, the SAT are interpreted as isotopically juvenile, arc terranes accreted to the Archaean core of the Wyoming craton along the Oregon Trail structural belt at *c.* 2650–2615 Ma in present-day southern Wyoming (Chamberlain *et al.* 2003; Frost *et al.* 2006*b*; Grace *et al.* 2006). They may represent a long-lived active margin with widespread arc magmatism from 2720 to 2620 Ma (Frost *et al.* 1998; Wall 2004; Bowers & Chamberlain 2006) and associated supracrustal rocks (Frost *et al.* 2006*b*).

Since *c.* 2730 Ma, the Archaean rocks exposed in the Bighorn Mountains have remained at relatively high crustal levels (summarized in Frost & Fanning 2006) and avoided Proterozoic deformations that took place far along the craton's boundaries. They are intruded by a number of unmetamorphosed, Proterozoic mafic dyke swarms that are the result of far-field stresses from extensional events and coeval mantle-derived magmatism.

Prior to this research, K–Ar and Rb–Sr data (Condie *et al.* 1969; Heimlich & Armstrong 1972; Stueber *et al.* 1976) constrained the ages of these Proterozoic Bighorn Mountain dykes. Potential correlative mafic intrusions from other regions of the Wyoming craton have U–Pb ages of 2480–1870 Ma (see Fig. 1 for details and references). These repeated pulses of Proterozoic mafic magmatism may be due to the progressive rifting and breakup of Wyoming's ancestral landmass. The Superior craton contains numerous mafic magmatic events during this same interval, including many with robust palaeomagnetic data: the Matachewan dykes at *c.* 2450 Ma (Halls 1991), the Nipissing sills and Senneterre dykes at *c.* 2215 Ma (Buchan 1991; Buchan *et al.* 1993, 2000), the Biscotasing dykes at *c.* 2170 Ma (Buchan *et al.* 1993; Halls & Davis 2004), the Marathon dykes at *c.* 2125 and 2105 Ma (Buchan *et al.* 1996; Halls *et al.* 2008), the Fort Frances and Lac Esprit dykes at *c.* 2070 Ma (Halls 1986; Buchan *et al.* 1996, 2007) and the Minto dykes at *c.* 2000 Ma (Buchan *et al.* 1998), among others (Evans & Halls 2010). The large number of similarly aged magmatic pulses in Superior support a proximal relationship to Wyoming (Ernst & Bleeker 2010).

Tilt corrections can be calculated locally using bedding orientations of overlying Phanaerozoic sedimentary rocks or structural studies of the thrusted blocks. The uplifts have varying amounts of relief and outcrop style depending on rock type, exhumation history and possibly lower crustal structures (Barnhart *et al.* 2012). Recent glaciations in the high mountains (e.g. the central Bighorn Mountains) provide widespread pavement exposures of basement rocks, but in regions such as South Pass (Wind River Range), the foothill shrub-lands and sagebrush steppe provide little relief or exposure other than recently incised river valleys.

Methodology

U–Pb geochronology

Samples for geochronology were taken from the same outcrops and dykes as palaeomagnetic samples (Fig. 1). In most cases, samples were taken from the freshest region of the coarsest rock, often

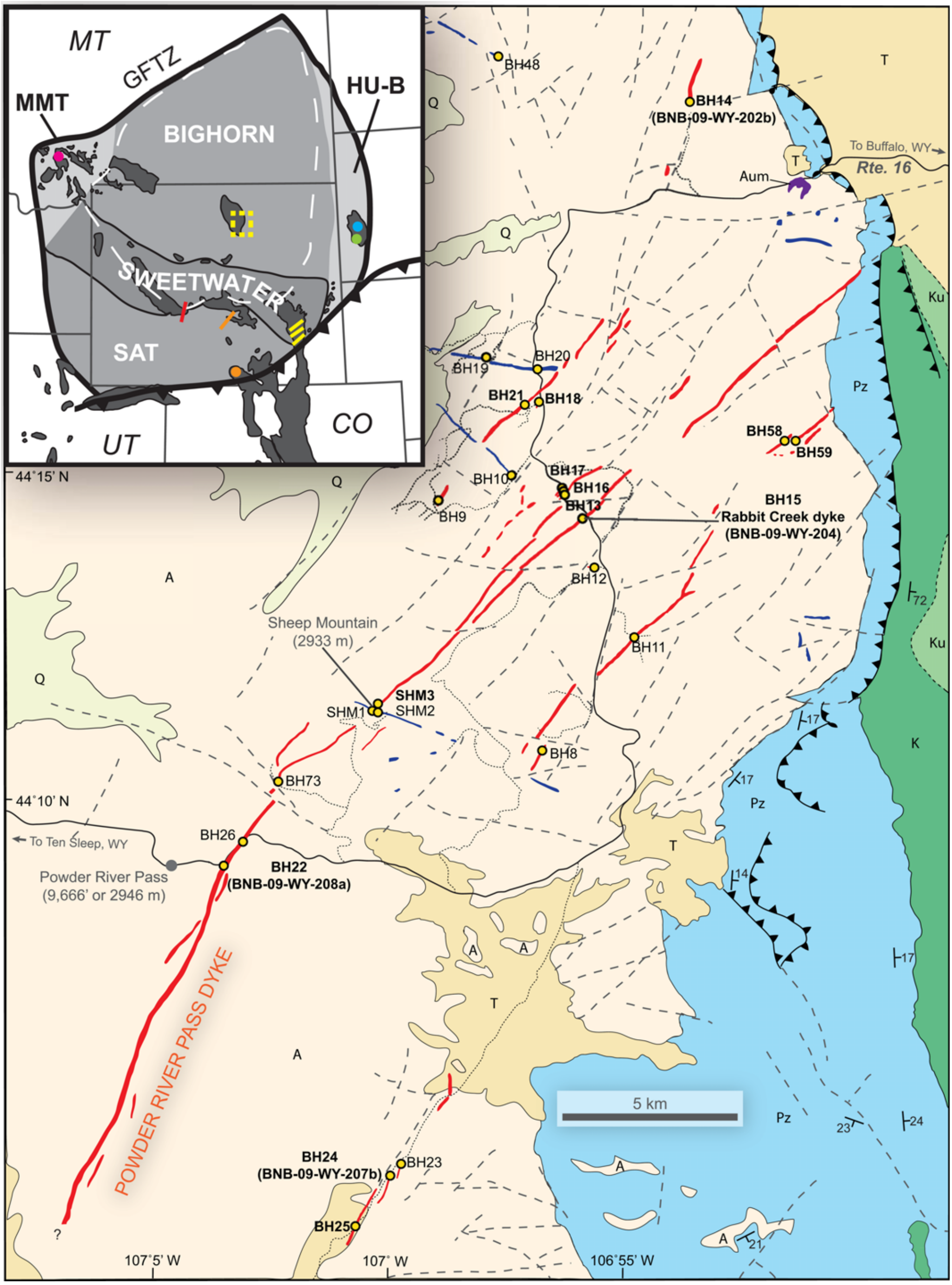

Fig. 1. Regional geological map with localities sampled for this study. Inset shows the location of the map (dotted yellow rectangle) with respect to state borders, including estimated extent of Wyoming craton (light grey) and outcrop of Precambrian rock (dark grey) (Foster *et al.* 2006). HU-B, Hartville uplift–Black Hills subprovince; GFTZ, Great Falls Tectonic zone; other subdivisions of the Wyoming craton are explained in the text. Inset also plots locations and trends of other dated mafic magmatic events in the early Proterozoic: the *c.* 2480 Ma Blue Draw metagabbro (blue dot) (Dahl *et al.* 2006), the South Pass dyke of the Wind River Range at *c.* 2164 Ma (red line) (Harlan *et al.* 2003

from the centre of spheroids resistant to weathering. The geochronological sample (BNB-09-WY-202b) for site T09BH14 was collected *c.* 13 m from the eastern margin of the *c.* 40 m-wide dyke. Sample (BNB-09-WY-204) for T09BH15 was collected within a linear meadow defined by the dyke, 10–12 m from the southern margin of the *c.* 40 m-wide dyke. For dyke T09BH24, a sample (BNB-09-WY-207b) was collected 10–15 m from the northern margin of the *c.* 50 m-wide dyke. Sample (BNB-09-WY-208a) for T09BH22 was taken *c.* 500 m NE of the palaeomagnetic sampling area, along a road-cut in the coarse diabasic portion of the >100 m-wide dyke. In the Wind River Range, the dyke of Harlan *et al.* (2003) was sampled (BNB-09-WY-210b) in its centre along the Sweetwater River.

All samples were crushed and separated using the Wilfley table technique of Söderlund & Johansson (2002) at the Institute of Geology, University of Lund, Sweden. All three 40–50 m-wide Rabbit Creek dykes from the Bighorn Mountains (202b, 204, 207b) yielded sufficient baddeleyites, allowing for the selection of high-quality grains. Four fractions were analysed for each sample, each fraction consisting of one to nine grains or crystal fragments (Table 1). Samples from large intrusions in both the Wind River Range (210b) and the Bighorn Mountains (208a) yielded baddeleyite crystals that were mostly clear. A subset of grains had a slightly mottled appearance on the surfaces; these were avoided for all but two of the analyses. Four fractions were analysed for each of these particular samples, comprising one to five crystals or crystal fragments.

Selected baddeleyite grains were spiked with a mixed $^{205}Pb–^{233}U–^{235}U$ tracer (ET535) and dissolved in 6 N hydrochloric acid in precleaned teflon microbombs at 180 °C for 30 h. Hydrochloric acid was used rather than hydrofluoric acid to minimize dissolution of any undetected zircon alteration rims (e.g. Rioux *et al.* 2010). Dissolved samples were evaporated and loaded onto Re filaments using H_3PO_4 and silica gel without any further chemical processing. Isotopic compositions of Pb and U (run as UO_2) were determined by peak-switching in a Daly-photomultiplier single collector on a Micromass S54 thermal ionization mass spectrometer at the University of Wyoming. Pb procedural blanks averaged 1–3 pg, and all measured common Pb was assigned to blank. U procedural blanks were consistently less than 0.2 pg. Mass discrimination of 0.198 ± 0.10%/amu for Pb was determined by replicate analyses of NIST SRM 981. U fractionation was determined internally for samples spiked with ET535. Concordia coordinates, intercepts, weighted means and uncertainties were calculated using MacPBDAT and ISOPLOT programs (based on Ludwig 1988, 1991) and the decay constants recommended by Steiger & Jäger (1977).

Geochemistry

The vast majority of sites consist of eight samples taken from the same outcrop of a single cooling unit (dyke). Specimens for geochemical analyses were taken from one of the eight samples used for palaeomagnetic measurements and were chosen from regions approximately one-third of a dyke width across in order to minimize effects from differentiated interiors or chilled margins (Table 2).

Rock samples were slabbed, crushed in a Bico Chipmunk jaw crusher, and ground to a fine powder in an agate ring mill. Whole-rock major and trace element contents were determined by fused-disc X-ray fluoresence spectrometry and solution-mode inductively coupled plasma mass spectrometry at the Ontario Geological Survey Geochemical Laboratories, Sudbury, Ontario. The precisions of the data, based on replicate analyses of samples and blind standards, along with representative analyses, are listed in Table 2. A subset of samples was selected for Sm–Nd isotopic analysis utilizing a ThermoFisher Triton T1 thermal ionization mass spectrometer at Carleton University (techniques of Cousens 2000). Nd isotope ratios are normalized to $^{146}Nd/^{144}Nd = 0.72190$. Analyses of the USGS standard BCR-1 yield $^{143}Nd/^{144}Nd = 0.512668 \pm 20$ ($n = 4$). Thirty runs of an internal Nd metal

Fig. 1. (*Continued*) and this study), *c.* 2110 Ma Bear Mountain dyke in the Ferris Mountains (orange line) (Bowers & Chamberlain 2006), *c.* 2090 Ma metagabbro in the Sierra Madre (orange dot) (Premo & Van Schmus 1989), *c.* 2060 Ma dyke in the Tobacco Root Mountains (pink dot) (Brady *et al.* 2004; Harms *et al.* 2004; Mueller *et al.* 2004), the *c.* 2010 Ma Kennedy dyke swarm in the Laramie Mountains (yellow lines) (Cox *et al.* 2000; Hark *et al.* 2008) and *c.* 1870 Ma sills and dykes in the Black Hills (green dot) (Redden *et al.* 1990). In the main figure, Precambrian mafic dykes are shown as red (Rabbit Creek dykes and Powder River Pass dyke) and blue (unknown age) linear polygons, with palaeomagnetic sites indicated by text labels (e.g. BH26) and yellow circles; sites that yielded reliable palaeomagnetic results are shown in bold. Toothed lines indicate the main thrusts that delineate the eastern Bighorn Mountains (teeth on hanging-wall side), while grey dashed lines indicate other faults. Roads are indicated with black (i.e. Route 16) and dotted black lines (US Forest Service roads). A, Granitic gneiss, Archaean; Aum, pyroxenite; Pz, Palaeozoic rocks (undifferentiated); Jurassic and Triassic rocks (665–725 m thickness); K, Lower Cretaceous rocks; Ku, Upper Cretaceous rocks; T, Tertiary sediments; and Q, Quaternary glacial deposits. The figure is based on field mapping from this study and existing maps (Heimlich *et al.* 1973; Hinrichs *et al.* 1990).

Table 1. *U–Pb TIMS baddeleyite data for samples BNB-09-WY-208a, -210b, -202b, -204, and -207b*

Sample	Mass	U	Sample Pb		Pbc	Pb*/Pbc	Th/U	$^{206}Pb/^{204}Pb$	$^{206}Pb/^{208}Pb$	Corrected atomic ratios $^{206}Pb/^{238}U$		$^{207}Pb/^{235}U$		$^{207}Pb/^{206}Pb$		Ages $^{206}Pb/^{238}U$	$^{207}Pb/^{235}U$	$^{207}Pb/^{206}Pb$	Rho		
	(µg)	(ppm)	(ppm)	(pg)	(pg)					(rad.)	%err.	(rad.)	%err.	(rad.)	%err.	Ma	Ma	Ma	err.		%disc.
BNB-09-WY-208a: Powder River Pass dyke (44.1545325°N, 107.0555169°W)										*Baddeleyite crystallization age = 2163.9 ± 7.1 Ma (MSWD = 2.4) 4 point upper intercept date*											
WY208a p6 dk 4g	0.32	101	40	13	1.4	9	0.04	599	82	0.3993	±0.52	7.4581	±0.9	0.1355	±0.63	2166	2168	2170	±11.0	0.73	0.22
WY208a p3 4g	1.2	152	60	72	4.7	15	0.15	993	23	0.3907	±0.21	7.2467	±0.49	0.1345	±0.38	2126	2142	2157.6	±6.7	0.68	1.7
WY208a p2 5g	1.8	80	34	61	5.4	11	0.72	633	4	0.3608	±0.26	6.6326	±0.75	0.1333	±0.6	1986	2064	2142.4	±10.5	0.69	8.49
WY208a p8 mt 1g	0.33	65	24	8	0.9	9	0.09	570	37	0.3629	±0.43	6.7346	±1.08	0.1346	±0.85	1996	2077	2158.7	±14.9	0.67	8.76
BNB-09-WY-210b: Wind River–South Pass dyke (42.4154436°N; 108.5145092°W)										*Baddeleyite crystallization age = 2164.1 ± 7.3 Ma (MSWD = 1.5) 3 point upper intercept date*											
*WY210b p6 2g	0.77	170	67	51	2.1	24	0.07	1538	53	0.3965	±0.21	7.3423	±0.43	0.1343	±0.32	2153	2154	2155.1	±5.6	0.68	0.13
WY210b p7 3g	0.77	62	25	19	1	19	0.16	1223	21	0.3936	±0.2	7.3214	±0.5	0.1349	±0.4	2139	2151	2162.9	±7.0	0.65	1.27
WY210b p5 3g	0.77	359	138	106	5.8	18	0.22	1139	15	0.3708	±0.22	6.8148	±0.54	0.1333	±0.43	2033	2088	2141.9	±7.5	0.66	5.92
WY210b p4 4g	0.77	112	37	29	1.7	17	0.09	1117	33	0.3336	±0.45	6.0458	±0.71	0.1314	±0.49	1856	1982	2117.2	±8.5	0.74	14.19
BNB-09-WY-202b: 'French Creek' diabase dyke (44°20.752′N; 106°53.721′W)										*Baddeleyite crystallization age = 2155.9 ± 2.9 Ma (MSWD = 0.11) 4 point weighted mean $^{207}Pb/^{206}Pb$ date*											
WY202b p1 4g	0.6	261	100	60	3	19	0.06	1253	53	0.3881	±0.14	7.1942	±0.38	0.1344	±0.31	2114	2136	2156.7	±5.4	0.67	2.32
WY202b p2 4g	0.6	306	119	71	12	6	0.06	399	56	0.3911	±0.31	7.2562	±1.15	0.1346	±0.95	2128	2143	2158.5	±16.5	0.75	1.67
WY202b p3 8g	0.6	351	137	83	7	11	0.09	732	36	0.3909	±0.21	7.2437	±0.64	0.1344	±0.52	2127	2142	2156.3	±9.0	0.69	1.6
WY202b p5 4g	0.68	108	43	29	1	27	0.11	1758	32	0.3931	±0.23	7.2806	±0.35	0.1343	±0.22	2137	2146	2155.2	±3.9	0.77	0.98
BNB-09-WY-204: 'Rabbit Creek' diabase dyke (44°14.23′N; 106°55.945′W)										*Baddeleyite crystallization age = 2154.2 ± 2.2 Ma (MSWD = 0.38) 4 point weighted mean $^{207}Pb/^{206}Pb$ date*											
WY204 p2 4g	0.9	268	104	94	10	10	0.08	649	44	0.3913	±0.19	7.2641	±0.7	0.1346	±0.58	2129	2144	2159.2	±10.1	0.74	1.65
WY204 p4 6g	1.2	61	24	29	1	24	0.12	1528	30	0.3962	±0.21	7.3352	±0.37	0.1343	±0.27	2152	2153	2154.6	±4.7	0.71	0.17
WY204 p6 6g	1.81	42	17	30	1	21	0.08	1403	42	0.3962	±0.21	7.3306	±0.39	0.1342	±0.29	2151	2153	2153.6	±5.0	0.69	0.12
WY204 p7 5g	1.2	81	31	38	1	28	0.06	1783	58	0.3861	±0.15	7.1455	±0.26	0.1342	±0.18	2105	2130	2153.8	±3.2	0.72	2.66
BNB-09-WY-207b: 'Dike C'† near Hazelton Peak (44°4.182′N; 106°59.978′W)										*Baddeleyite crystallization age = 2157.7 ± 3.6 Ma (MSWD = 0.08) 4 point weighted mean $^{207}Pb/^{206}Pb$ date*											
WY207b p3 9g	2.71	88	34	93	20	5	0.05	321	68	0.3946	±0.32	7.3198	±1.43	0.1345	±1.19	2144	2151	2158	±20.7	0.81	0.75
WY207b p4 6g	1.2	38	15	18	2	11	0.14	701	26	0.3963	±0.27	7.3405	±0.72	0.1343	±0.57	2152	2154	2155.5	±10.0	0.67	0.2
WY207b p5 6g	1.81	47	19	33	1	26	0.08	1677	44	0.3982	±0.17	7.3856	±0.33	0.1345	±0.25	2161	2159	2157.9	±4.4	0.68	−0.15
WY207b p7 6g	1.81	14	5	10	1	10	0.14	645	25	0.3931	±0.43	7.296	±0.81	0.1346	±0.58	2137	2148	2158.9	±10.1	0.72	1.17

Locations in WSG84 coordinates. All date errors are reported at a 95% confidence interval. p, Pick identifier; dk, dark; mt, mottled; g, number of grains. Sample Pb, sample Pb (radiogenic + initial) corrected for laboratory blank; Pbc, total common Pb (blank plus sample initial Pb); Pb*/Pbc, radiogenic Pb to total common Pb (blank + initial); corrected atomic ratios, measured $^{206}Pb/^{204}Pb$ corrected for mass discrimination and tracer, all others corrected for blank, mass discrimination, tracer and initial Pb; %err., 2σ errors in per cent. $^{207}Pb/^{206}Pb$ errors (err) are $\pm 2\sigma$; Rho, $^{206}Pb/^{238}U$ vs $^{207}Pb/^{235}U$ error correlation coefficient; % disc., per cent discordant. Baddeleyite dissolution and chemistry were adapted from methods developed by Krogh (1973); Parrish *et al.* (1987) and Rioux *et al.* (2010). One dissolution of each sample was processed through ion exchange columns to separate Hf, but the others were evaporated and loaded without chemical processing. All of the common Pb was assigned to blank, although measured blanks were between 2 and 0.6 pg. Isotopic composition of the Pb blank was estimated as 18.75 ± 1, 15.652 ± 0.6 and 38.81 ± 0.2 for 206/204, 207/204 and 208/204, respectively. U blanks were consistently less than 0.2 pg. Initial Pb isotopic compositions were estimated from Stacey & Kramers (1975) model. The decay constants used by PBDAT and MacPBDAT are those recommended by the IUGS Subcommission on Geochronology (Steiger & Jäger 1977): 0.155125×10^{-9}/year for ^{238}U, 0.98485×10^{-9}/year for ^{235}U and present-day $^{238}U/^{235}U = 137.88$.

*Excluded from linear regression.

†'Dike C' refers to the original designation of this dyke by Heimlich *et al.* (1973).

Table 2. *Geochemical results for dykes from the Bighorn Mountains*

d, *w*	BH13 3.1,7.5	BH14 9,30	BH15 4,40	BH16 0.7,2.9	BH17 1.7,4.8	BH21 1.5,6.7	BH22 7,70 +	BH24 2,40 +	BH25 2.5,40	BH58 4,13	BH59 5,20	Int. Std	1σ
SiO_2	48.66	48.94	48.82	48.64	48.95	48.69	49.05	48.57	48.49	48.16	48.50	50.5	0.36
TiO_2	1.55	1.51	1.50	1.58	1.36	1.61	1.36	1.15	1.22	1.15	1.17	2.45	0.03
Al_2O_3	13.51	15.06	13.65	13.44	13.60	13.05	13.58	14.95	14.04	15.37	14.57	13.64	0.09
$Fe_2O_3^T$	16.38	15.26	15.81	16.33	15.47	16.66	15.67	13.70	14.83	13.42	14.32	13.41	0.05
MnO	0.23	0.21	0.22	0.24	0.23	0.23	0.23	0.20	0.21	0.20	0.21	0.24	0
MgO	5.71	5.25	6.15	5.98	6.58	5.99	6.56	6.73	7.11	5.89	7.19	4.02	0.05
CaO	9.69	10.16	9.89	9.84	10.03	9.88	9.85	11.07	11.11	10.98	11.21	7.47	0.11
Na_2O	2.12	2.37	2.06	2.04	2.02	2.03	2.11	2.10	2.02	2.13	2.13	3.16	0.05
K_2O	0.67	0.40	0.55	0.56	0.66	0.45	0.81	0.64	0.28	0.57	0.20	1.85	0.04
P_2O_5	0.16	0.14	0.14	0.16	0.13	0.15	0.12	0.07	0.08	0.08	0.08	1.17	0.01
LOI	0.98	0.69	0.82	0.74	0.55	0.54	0.54	0.77	0.38	1.18	0.19	1.62	0.33
Total	99.66	99.99	99.62	99.55	99.58	99.28	99.88	99.96	99.78	99.13	99.77	99.53	–
Mg#	0.434	0.431	0.461	0.446	0.483	0.442	0.479	0.519	0.513	0.491	0.525	0.397	0
V	311	323	335	336	297	348	317	284	297	285	284	337	13
Cr	161	157	156	135	172	143	156	185	195	135	200	19	5
Co	51.6	49.7	52.8	53.8	53	52.4	55.4	50.2	54.6	46.4	54.4	29	3
Ni	76	75	91	85	95	79	94	100	110	76	116	12	3
Zn	136.8	129.4	126.8	130.8	124.8	125.4	135.6	96.7	106.8	109.2	103.0	133	7
Rb	28.3	10.9	21.9	23.9	23.9	16.1	32.0	22.6	11.2	13.8	3.6	40	3
Sr	128	140	133	128	124	115	135	167	137	162	138	408	5
Y	31.4	28.4	29.4	30.2	27.8	30.3	26.6	17.6	19.2	17.3	18.0	47	4
Zr	115	106	108	112	98	107	92	60	66	59	62	149	5
Nb	6.0	5.5	5.5	5.9	5.2	5.7	4.8	3.1	3.3	3.0	3.1	8	1
Ba	120	97.9	181.1	160.6	107.4	110.7	111.9	100.7	88.4	91.3	41.5	2202	143
La	9.38	8.5	8.6	8.7	7.92	8.6	7.58	4.11	4.46	4.06	4.21	26.68	0.55

(*Continued*)

Table 2. *Continued*

d, *w*	BH13 3.1,7.5	BH14 9,30	BH15 4,40	BH16 0.7,2.9	BH17 1.7,4.8	BH21 1.5,6.7	BH22 7,70 +	BH24 2,40 +	BH25 2.5,40	BH58 4,13	BH59 5,20	Int. Std	1σ
Ce	22.65	20.5	20.55	21.18	19.11	20.92	18.36	10.3	11.09	10.27	10.88	58.55	0.21
Pr	3.23	3	2.98	3.1	2.78	3.06	2.64	1.6	1.79	1.63	1.68	8.41	0.08
Nd	15.23	13.82	13.91	14.48	12.93	14.37	12.42	8.25	8.77	7.97	8.39	39.39	0.42
Sm	4.28	3.8	3.92	4.01	3.62	4.05	3.52	2.51	2.81	2.48	2.61	9.47	0.06
Eu	1.38	1.3	1.3	1.34	1.22	1.32	1.17	1	1.06	0.99	1.03	3.82	0.1
Gd	5.1	4.69	4.75	4.85	4.38	4.92	4.26	3.17	3.44	3.12	3.22	9.92	0.35
Tb	0.869	0.772	0.782	0.818	0.746	0.835	0.723	0.524	0.578	0.52	0.531	1.45	0.02
Dy	5.68	5.14	5.28	5.4	4.89	5.56	4.79	3.39	3.65	3.27	3.44	8.81	0.16
Ho	1.17	1.06	1.08	1.12	1.03	1.17	0.99	0.68	0.73	0.67	0.7	1.76	0.01
Er	3.55	3.17	3.19	3.36	3.08	3.45	3.03	1.95	2.1	1.9	1.98	4.94	0.01
Tm	0.508	0.46	0.466	0.484	0.444	0.496	0.443	0.273	0.295	0.266	0.273	0.68	0.01
Yb	3.33	3.01	3.03	3.18	2.92	3.21	2.90	1.75	1.89	1.71	1.74	4.33	0.06
Lu	0.5	0.45	0.45	0.47	0.44	0.49	0.43	0.25	0.27	0.25	0.26	0.64	0.02
Rb	28.29	10.91	21.91	23.93	23.92	16.12	31.96	22.57	11.16	13.77	3.6	41.74	0.46
Sr	128	140	133	128	124	115	135	167	137	162	138	414.61	9.4
Nb	5.96	5.5	5.53	5.86	5.21	5.66	4.81	3.07	3.31	2.97	3.12	7.58	0.22
Cs	0.96	0.36	0.53	0.48	0.63	1.07	0.6	0.86	0.83	0.65	0.21	1.73	0.04
Hf	3.05	2.85	2.89	3.02	2.65	2.93	2.49	1.71	1.83	1.68	1.72	4.09	0.05
Ta	0.4	0.4	0.4	0.4	0.3	0.4	0.3	0.2	0.2	0.2	0.2	0.47	0.03
Th	1.08	1.02	0.97	1.02	0.91	1.04	0.9	0.37	0.41	0.37	0.4	4.08	0.32
U	0.28	0.25	0.26	0.26	0.23	0.29	0.22	0.09	0.09	0.1	0.1	1.52	0.11
Sc	39.5	36.8	41.1	40.5	39.4	41.7	41.4	34.3	34.9	32.3	33.3	37.6	0.5
Pb	1.7	1.8	3.2	2.9	1.3	1.2	3.2	1	3.4	0.8	0.6	6.95	0.07

Major oxides by XRF in wt%, trace elements by ICP-MS in weight ppm, and LOI, loss on ignition. Mg#, Mg/(Mg + Fe^{2+}). Int. Std, Standard basalt from Lake Tahoe, California submitted as blind standard. Precision is shown in final column, 1σ (SD). *d*, Estimated distance (in metres) of sample from the closest margin of the dyke; *w*, total width of dyke (in metres).

Table 3. *Isotopic data for selected Bighorn dykes*

	Sm (ppm)	Nd (ppm)	^{147}Sm/^{144}Nd	^{143}Nd/^{144}Ndm	2σ	ε_{Nd} pres	^{143}Nd/^{144}Nd (T)	ε_{Nd} (T)	T_{dm} (Ma)
BH13	4.25	15.12	0.1698	0.512312	0.000014	−6.35	0.509903	1.12	2757
BH22	3.95	13.94	0.1714	0.512334	0.000012	−5.92	0.509892	1.12	2784
BH24	2.48	7.98	0.1879	0.512625	0.000012	−0.25	0.509954	2.20	2852
BH58	2.41	7.74	0.1879	0.512605	0.000013	−0.65	0.509938	1.81	2965

m, Measured; pres, present day; T, ratio at time of crystallization at 2155 Ma, based on U–Pb ages (this study); T_{dm}, depleted mantle model age.

standard average ^{143}Nd/^{144}Nd = 0.511823 ± 12, corresponding to a La Jolla value of 0.511852 based on comparative runs (May 2008–2011). Isotopic data are listed in Table 3.

Palaeomagnetism

Sampling was accomplished in the field using a portable, gasoline-powered core drill. Cylindrical samples were oriented using both a magnetic and a sun compass, except in the case of sites T09BH18 and T10BH59 where only magnetic measurements were possible and a regional declination correction was used.

Only one baked-contact test was performed because exposures of the baked zones of county rock are very limited and often non-existent. Exposures of dyke intersections (for the purpose of baked-contact tests) also are extremely rare. Where intersections are mapped there are often wetlands or lakes, both in the alpine and conifer forests. In the field, dykes are typically either slightly more resistant, forming minor topographic highs, or are devoid of trees, forming long meadows with small resistant diabase knobs protruding through the soil.

Samples were prepared and measured at the Yale palaeomagnetic facility, which is equipped with a 2G Enterprises™ SQuID rock magnetometer and an automatic sample changer system (Kirschvink *et al.* 2008) with a background noise sensitivity of 5×10^{-12} A m^2 per axis. The samples were stored within a magnetically shielded room (<100 nT residual field) and were demagnetized and measured with additional magnetic shielding. After measurement of the natural remanent magnetization, the samples were first demagnetized using liquid nitrogen immersion (Halgedahl & Jarrard 1995), greatly reducing the masking remanence of multi-domain magnetite by cycling through magnetite's Verwey crystallographic transition at 77 K (Muxworthy & Williams 2006) in a near-zero magnetic field. Subsequently, the samples were thermally demagnetized in small temperature increments within a magnetically shielded furnace and controlled nitrogen atmosphere. Results were analysed using the free computer software packages described by Jones (2002) and Cogné (2003), which use principal component analysis to calculate least-squares fits of magnetic components (Kirschvink 1980) and palaeomagnetic poles.

Structural corrections

Large-scale thrust faults during the Laramie Orogeny carried exposures of the Wyoming craton to the surface. In most cases, small outliers of Phanaerozoic strata still remain on top of the uplifted blocks and can be used to assess for basic tilt corrections. In the Bighorn Mountains, Phanaerozoic strata indicate that tilt corrections are small (<10°), especially when sampling is restricted towards the stable interior of the uplift (Osterwald 1978; Hoy & Ridgway 1997). Large rotations are mainly restricted to the steep frontal limbs of uplifts where fold trends curve (Weil *et al.* 2009). The Wind River Range has both Phanaerozoic outliers and structural studies of its main thrust fault (Smithson *et al.* 1979, 1980), and at its core requires no more than 15° of tilt correction. Still, the sampling localities of Harlan *et al.* (2003) derive from the far-SE portion of the uplift, where the dramatically straight but tilted NE boundary of the Wind River Range curves 30° to the north. This suggests an additional assessment of some vertical-axis rotations resulting from different amounts of fault displacement along the Wind River thrust, which decreases towards the NW and SE ends of the uplift. We assume that any large vertical-axis rotations are restricted to the edges of thrusted blocks while the central cores of the large basement uplifts experienced only small horizontal-axis tilting, modelled well by Laramide structural and seismic studies (Brown 1993). Palaeomagnetic directions obtained from the Triassic Chugwater Formation along the margin of multiple uplifts in Wyoming agree remarkably well after only minor tilt corrections according to local bedding

(Collinson & Runcorn 1960), suggesting that no major uplift-scale vertical-axis rotations occurred in the basement hanging walls throughout Wyoming.

In general, dykes intrude along sub-vertical planes into the crust and are good indicators, by themselves, of major systematic tilting (unless tilting occurred perpendicular to the trend of a vertical dyke). Nonetheless, each palaeomagnetic site is assessed for tilting independently, taking into account local structural studies or nearby outliers of sedimentary rock. In addition, apatite (U–Th)/He thermochronology of the Bighorn Mountains confirms that relative differences in exhumation rates across the range were small, with only minor regional tilting of the thrust block (Crowley *et al.* 2002).

Results

U–Pb geochronology

The northernmost dyke at French Creek (BNB-09-WY-202b; palaeomagnetic site BH14) yields a weighted mean $^{207}Pb/^{206}Pb$ age of 2155.9 $\pm$ 2.9 Ma (all uncertainties are 2σ unless stated otherwise). The more northeasterly trending Rabbit Creek dyke (−204, palaeomagnetic site BH15) yields a $^{207}Pb/^{206}Pb$ age of 2154.2 $\pm$ 2.2 Ma, while the southern dyke (−207b, palaeomagnetic site BH24) in the Hazelton Peak area yields a $^{207}Pb/^{206}Pb$ age of 2157.7 $\pm$ 3.6 Ma (Fig. 2). Given these uncertainty envelopes, all three dated dykes appear to belong to the same magmatic event, and we cannot currently resolve whether the NE-trending Rabbit Creek dyke is slightly younger or older than the more NNE-trending dykes. Cross-cutting relationships are difficult to obtain because most locations where dykes intersect are more deeply eroded and covered by wetlands or lakes. Therefore we group all three dykes (202b, 204 and 207b) into the same event, possibly lasting from 2161 to 2152 Ma in multiple pulses with slightly different trends.

Geochronological results from the Powder River Pass dyke in the Bighorn Mountains (−208a) and from the South Pass dyke in the Wind River Range (−210b) are overlapping in error, with upper intercept ages of 2163.9 $\pm$ 7.1 and 2164.1 $\pm$ 7.3 Ma, respectively (Fig. 3). If we assume that these two dykes are part of the same intrusion, then their data may be combined to calculate a single age of 2164.0 $\pm$ 5.1 Ma (Fig. 4). Comparing this with the $^{207}Pb/^{206}Pb$ ages calculated for the smaller Rabbit Creek dykes from the Bighorn Mountains (202b, 204, 207b), we can see that at a 95% confidence interval some of the individual ages overlap but are different enough to suggest that there were at least two distinct pulses of magmatism in the time interval from 2152 to 2171 Ma. This is particularly evident when comparing the individual ages of BH15 (−204) and BH22 (−208a), which are distinct at a 95% confidence interval. For that reason we name the younger group of dykes the Rabbit Creek swarm, after the drainage along the northern margin of BH15 (−204).

Four of the five dated samples had at least one analysis that overlapped concordia within error (Table 1). Results for the three smaller Bighorn dykes are all <3% discordant and form relatively tight clusters with zero age lower intercepts (Table 1, Fig. 2), so both upper intercept and weighted-mean $^{207}Pb/^{206}Pb$ dates yield the same means within error. The weighted-mean $^{207}Pb/^{206}Pb$ dates are interpreted as the best estimates of crystallization ages for these three samples. Results from the 100 m-wide dykes from Powder River (−208a) and South Pass (−210b) display a range of discordance from 0 to 14% (Table 1, Fig. 3) and lower intercepts of 340 and 480 Ma, respectively. For these samples, the upper intercept dates are interpreted to be the best estimates of magmatic ages as they include most of the analyses. One analysis from the South Pass dyke (p6) does not lie on the chord defined by the other three analyses and was excluded from the linear regression, even though it is the least discordant. Our new data for the South Pass dyke are significantly less discordant than those of Harlan *et al.* (2003). They lead to a more precise date and permit this intrusion to be linked to the Powder River Pass dyke.

Geochemistry

All samples are basaltic in composition, with SiO_2 contents (recalculated to a volatile-free basis) between 48.7 and 49.3% (weight per cent). The dyke samples can be subdivided into at least two groups, referred to below by their locations within the swarm: southeastern and northwestern. Samples BH24, BH25, BH58 and BH59 from the southeastern dyke set have the highest MgO (7.2–6.8%) and lowest SiO_2, TiO_2, P_2O_5 and incompatible trace element abundances (e.g. Th, Nb, REE; Fig. 5). Samples BH13 to BH17, as well as BH21 and BH22 from the northwestern dyke set, have lower MgO (6.6–5.3%) and higher SiO_2, TiO_2, P_2O_5 and incompatible trace elements (Table 3). In the latter group, concentrations of most incompatible trace elements are negatively correlated with Mg# (atomic $Mg/(Mg + Fe^{2+})$). The geochemical distinction between the southeastern and northwestern dyke sets is evident in the primitive mantle-normalized incompatible element plot of Figure 6. There is no overlap between patterns from the two groups, and the patterns are different for each group.

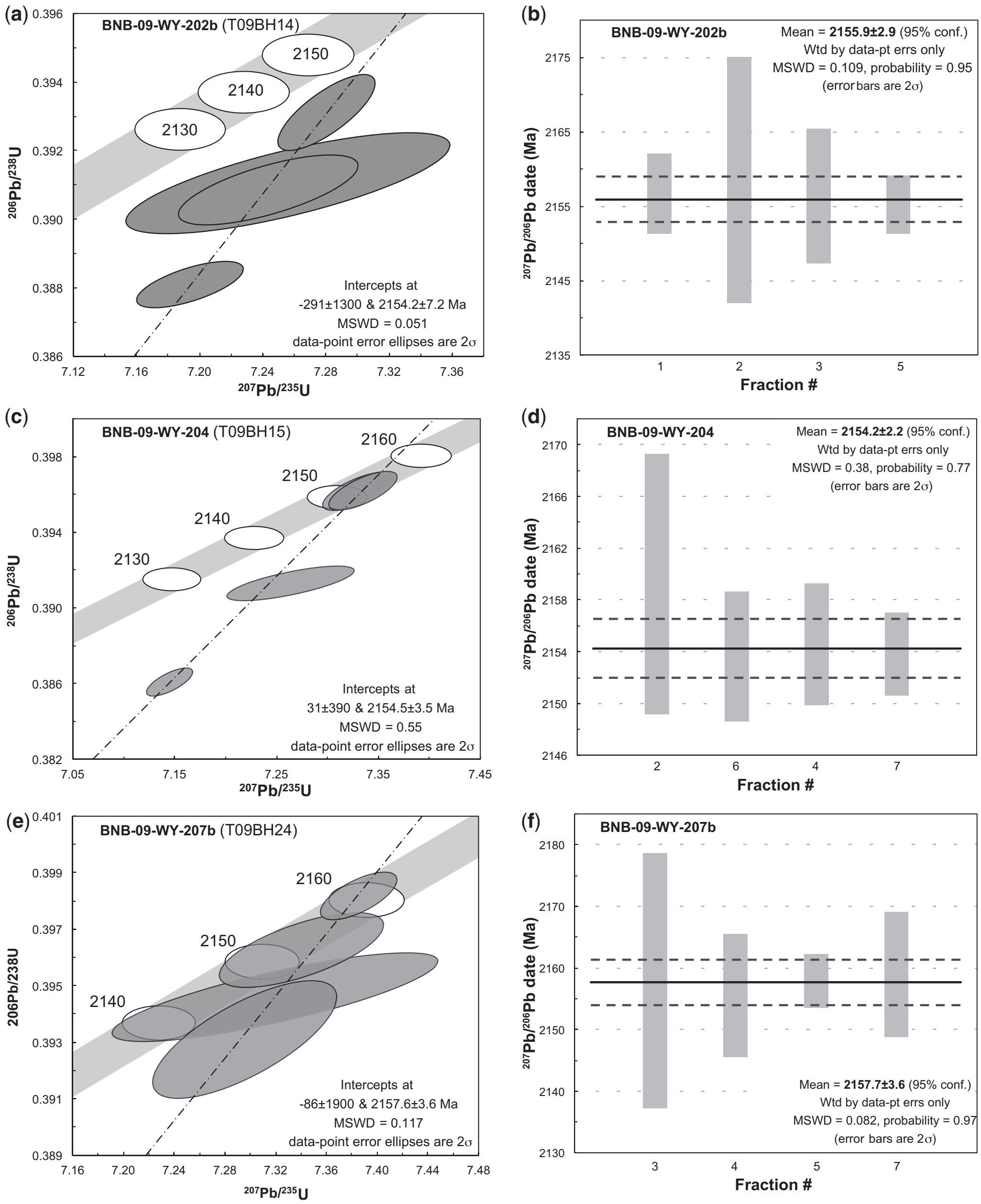

Fig. 2. U–Pb geochronological results for samples BNB-09-WY-202b, -204 and -207b. (**a**), (**c**) and (**e**) show concordia diagrams for each sample, including upper intercept ages; bracketed precisions include decay constant uncertainties. Mean square weighted deviations (MSWD) are normalized chi-squared probability tests with expectation values of *c.* 1. (**b**), (**d**) and (**f**) show $^{207}Pb/^{206}Pb$ ages of the different baddeleyite crystal fractions analysed for each dyke, including their weighted means, which are preferred because of their agreement with intercept ages and more precise error interval. All error intervals are shown as 2σ.

The southeastern dykes have lower La/Sm_{pmn} (pmn = primitive mantle-normalized) and a slight positive Eu anomaly and lack the enrichment in Th and U relative to Nb that is evident in the northwestern dykes. Both dyke sets are depleted in P relative to the REE.

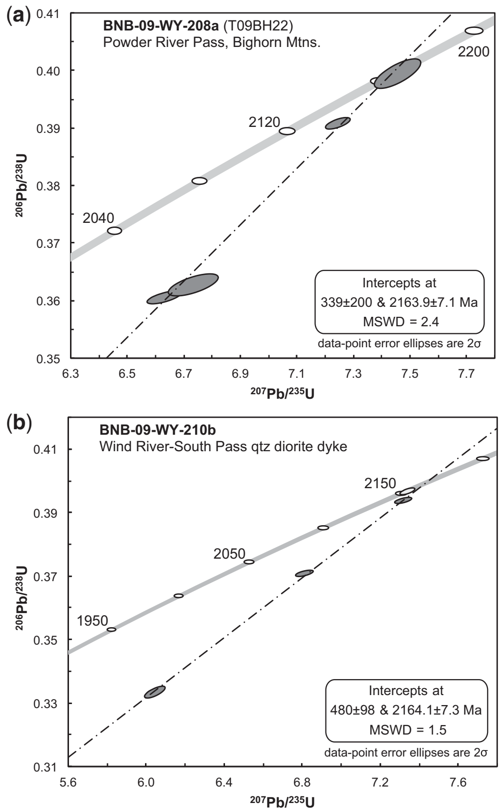

Fig. 3. U–Pb geochronological results for samples (**a**) BNB-09-WY-208a and (**b**) BNB-09-WY-210b are up to 14% discordant and rely on upper intercept fits for magmatic crystallization ages. A concordant analysis from BNB-09-WY-210b (pale grey) is excluded from the age estimation because it plots off the linear regression of the other three analyses.

The two dyke groups are also distinct isotopically. Two southeastern dykes have ε_{Nd} values between +1.8 and +2.2, whereas two northwestern dykes have ε_{Nd} of +1.1.

Palaeomagnetism

We sampled 19 sites in 15 dykes that were probably part of the Rabbit Creek swarm according to similar dyke orientations and proximity (Table 4); 13 sites yielded stable palaeomagnetic data (shown in bold font, Fig. 1). Six sites yielded data that were scattered and inconsistent because magnetizations either were unstable even at low temperatures (<300 °C) or had been remagnetized by a lightning strike. The Rabbit Creek palaeomagnetic pole is calculated from nine sites (or cooling units) that produced internally consistent thermal demagnetization behaviour (Figs 7 & 8), yielding a mean thermoremanent magnetization (TRM) confirmed to be primary through a positive baked-contact test (Everitt & Clegg 1962; Schwarz *et al.* 1985). This test was performed on the Sheep Mountain dyke intruding a probably Archaean, NW-trending mafic dyke (Figs 9 & 10). The Sheep Mountain dyke is not precisely a member of the Rabbit Creek swarm, rather it correlates to the slightly older South Pass dyke. Nonetheless, this positive baked-contact test verifies the primary nature of the Rabbit Creek dyke pole because their magnetizations and ages are so close to each other. Four sites from the east-central portion of the study area (BH13, BH16, BH17, BH59) yielded samples possessing only one direction of magnetization that persisted until the unblocking temperature of magnetite was surpassed. All other sites produced a mixture of sample behaviour, including frequent removal of magnetizations at temperatures below 500 °C that show little consistency within or between sites (Fig. 8). When compared, these components below *c.* 500 °C appear to be uniformly distributed on an equal-area plot; therefore they are probably the result of multi-domain magnetite that acquired viscous remanent magnetization (VRM). At two sites (BH22 and BH24) a component was demagnetized below 200 °C that appears very similar to the present local field, which is probably a chemical remanent magnetization held by goethite.

The primary magnetization typically unblocked between 550 and 575 °C. Some samples unblocked through a wider range of temperatures (from 500 to 565 °C), allowing a least-squares fit using more data points (Fig. 8). In some cases, smaller unblocking temperature ranges are the result of overlapping magnetization components from a wider range of magnetite grain sizes with small VRM components unblocking below *c.* 550 °C. This may be the result of different sampling locations across the width of a dyke, in which grain sizes can vary greatly. Grain size variation can be even more prevalent in wider dykes, which may be the cause of unblocking temperature variation in the Rabbit Creek swarm, where dyke widths vary from 3 to 50 m and sampling is limited to certain portions of dykes that are best exposed.

The high temperature magnetization is proved as primary with a positive baked-contact test sampled into an older Archaean(?) dyke (SHM2) near the summit of Sheep Mountain (Figs 1 & 9). Thermal demagnetization of samples adjacent (SHM1) to the Sheep Mountain dyke (SHM3), probably a continuation of the Powder River Pass dyke, reveal two distinct components: a 'baked' TRM indistinguishable from that obtained from site SHM3 and a stable 'unbaked' magnetization farther away from the Sheep Mountain dyke. Sample SHM2-5 is

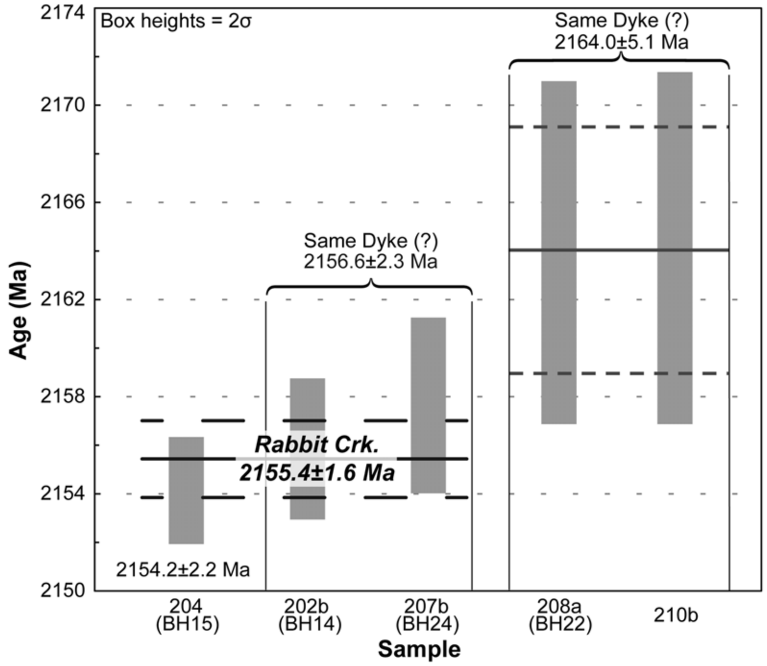

Fig. 4. Summary of U–Pb ages for the Rabbit Creek and Powder River–South Pass dykes. Sample IDs are given in terms of geochronological sample numbers with corresponding palaeomagnetic site for the same dyke in parentheses. Mean ages are calculated hypothesizing that 202b and 207b are a single dyke, and 208a (Bighorn Mountains-Powder River Pass dyke) and 210b (Wind River Range-South Pass dyke) are similarly from a single dyke. Also shown is a weighted mean of all Rabbit Creek age estimates.

completely baked by the Sheep Mountain dyke at *c.* 5 m away, with no indication of any remaining Archaean magnetization (Fig. 10). Samples taken at *c.* 6.5 m (SHM1-7), *c.* 9 m (SHM1-8), and *c.* 15 m (SHM1-9) show a hybrid zone behaviour in which the older ‘unbaked’ magnetization was not completely overprinted by heat from the Sheep Mountain dyke (Fig. 10), resulting in two components that coexist in the same sample within different temperature ranges. Sample SHM1-7 contains a high-temperature Archaean(?) magnetization (568–573 °C) in addition to a baked partial TRM that unblocked at a lower temperature range (500–565 °C). Sample SHM1-8 also contains both magnetizations; however, the high-temperature (unbaked) component extends into lower temperatures (560–576 °C), the result of being *c.* 2.5 m farther away from the heat source (Fig. 10). Sample SHM1-9 retained a baked magnetization at similar temperatures to sample SHM1-8. Any indication of a baked component disappears at *c.* 20 m from the Sheep Mountain dyke in sample SHM1-10, which records only an older, unbaked component. The baked zone, where temperatures exceeded *c.* 530 °C in samples SHM1-9, extends about one-third of a dyke width from the Sheep Mountain dyke, within the predicted range of cooling models (Delaney 1987). The survival of the unbaked magnetization in sample SHM1-7 indicates that *c.* 6.5 m away from the Sheep Mountain dyke temperatures never exceeded *c.* 568 °C. This is unexpected considering the large size of the Sheep Mountain, but this phenomenon can be explained in a couple of ways. The ambient host rock temperatures could have been fairly low (shallow in the crust), shifting contact temperatures lower and effectively shrinking the size of the baked zone. Another possibility has to do with the sample locality and outcrop on Sheep Mountain. Owing to limited exposure, the estimated distances of samples from the Sheep Mountain dyke margin (Fig. 10) were measured from the projected contact of the dyke (Fig. 9). It is possible that the dyke is not a perfect plane as assumed, and that it changes direction near SHM1, causing our length estimates to shift by metres. A dextral fault could have the same effect if it were to pass between the Sheep Mountain dyke and site SHM1, making SHM1 appear closer to the margin of the Sheep Mountain dyke. This seems plausible considering that the intrusion is next exposed over 700 m to the SE, making it difficult to judge if there has been any offset. Regardless,

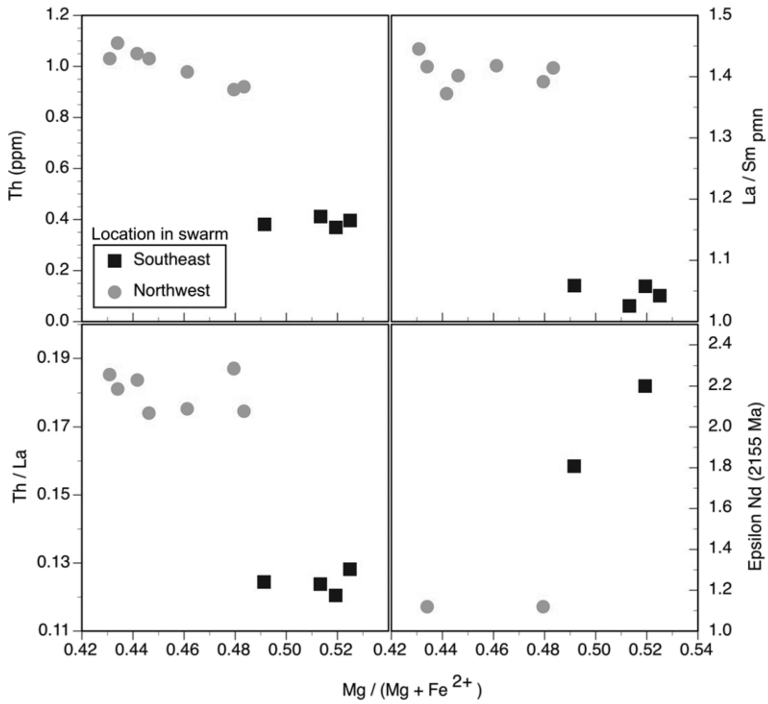

Fig. 5. Th concentration, La/Sm$_{pmn}$, Th/La and ε_{Nd} v. Mg# (Mg/(Mg + Fe^{2+}) for Rabbit Creek dykes. Symbols distinguish dykes by location within the swarm.

the identification of baked, hybrid and unbaked zones adjacent to the Sheep Mountain dyke comprise a complete and positive baked-contact test, affirming that the remanence was acquired at the time of dyke emplacement and cooling.

The unbaked direction is similar to magnetizations obtained from other likely Archaean dykes in the southern Bighorn Mountains, though this unbaked magnetization is considerably different from that derived from the 2.71 Ga Stillwater complex (Selkin *et al.* 2008). The unbaked direction may be somewhat younger than the Stillwater complex and possibly a thermoviscous remanent magnetization recorded through regional uplift and cooling during late Archaean accretion and plutonism on the southern margin of the craton.

Two sites from the large and differentiated Powder River Pass dyke (BH22 and SHM3) yielded stable palaeomagnetic data. Site BH22 was collected from the diabasic portion of the dyke, near sample BNB-09-WY-208a, along a quarried section of the dyke. Site SHM3 was collected in coarse leucogabbro near the summit of Sheep Mountain. Because this intrusion is of such unique size and mineralogy, we judge that it is very likely to be the only *c.* 2164 Ma dyke sampled in the Bighorns, with all other sites belonging to the Rabbit Creek swarm. Although its age is significantly different from the Rabbit Creek dykes, the Powder River Pass dyke has a very similar high-temperature magnetization to the rest of the dykes in the SE Bighorn Mountains. For that reason, the baked-contact test on the Powder River Pass dyke can be applied to the Rabbit Creek magnetization, especially because the intrusion slightly predates the Rabbit Creek dykes.

Structural corrections

Assessment for small structural corrections are necessary on both local and regional scales to account for the slight rotations of blocks that occurred during the Laramide Orogeny. Models of deformation during uplift (Hoy & Ridgway 1997) indicate that the basement was vertically thrust up 8–10 km on the eastern flank of the Bighorn Mountains. The same models also suggest that the core of the uplift remained sub-horizontal with negligible tilting of less than 5°. Towards the margin of the uplift, near the main basement thrust fault (less than 2 km away), more significant tilt corrections are required (Table 5). In the two areas where samples were collected 2–3 km from thrust faults (Sisters Hill and Clear Creek Thrusts, sites BH58, BH59 and BH14), we apply a 10° correction.

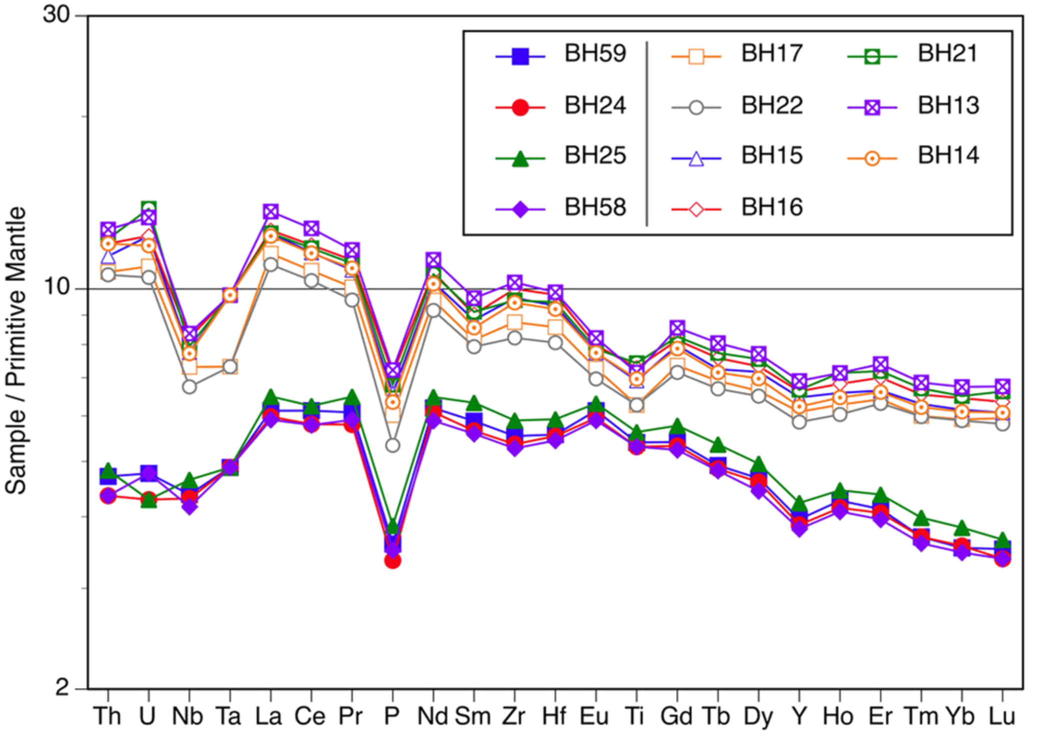

Fig. 6. Primitive mantle-normalized (Sun & McDonough 1989) trace element patterns for Rabbit Creek dykes. Only immobile elements are plotted. Filled symbols indicate the southeastern group of dykes.

Palaeomagnetic results from two dykes in the Bighorn Mountains (BH14 and BH24) are separated by *c.* 70° of declination from the mean results of all other Rabbit Creek dykes. After tilt corrections are applied to the palaeomagnetic dataset, the concentration and confidence interval of the Rabbit Creek mean direction are both improved, except for the outlying data from BH14 and BH24, which come into better agreement with each other, not the mean (Fig. 7). Along with their similar ages, this suggests that BH14 and BH24 might be the same dyke. Despite their difference geochemically as well as the difficulty in tracing them to each other in the field, they are approximately the same width and trend and are nearly along strike of each other. We exclude the palaeomagnetic data from these sites in the calculation of the Rabbit Creek palaeomagnetic pole because they are completely different from all other sites, even though they share similar and precise U–Pb ages along with stable palaeomagnetic behaviour. The primary palaeomagnetic remanence from dykes BH14 and BH24 probably records an excursion of the magnetic field that is not representative of Earth's dipolar field.

Results from the South Pass region (Harlan *et al.* 2003) require a tilt correction according to nearby Palaeozoic sediments to the north (Denson & Pipiringos 1974; Hausel 1991). In addition, the area near the dyke is sheared and faulted, causing the overall trend of the intrusion to appear more northerly. We propose that a lateral thrust ramp underlies the far southeastern edge of the Wind River thrust fault, causing *c.* 30° of counterclockwise (CCW) rotation of the basement, accommodated mostly by coplanar shearing of vertical Archaean metasediments. The angle of vertical-axis rotation that the South Pass region experienced is estimated from the change in strike of the northern boundary of the Wind River Range (Fig. 11). When the South Pass dyke is restored according to all Laramide rotations, it points towards the southern Bighorn Mountains, nearly along-strike with the Powder River Pass dyke. Between the South Pass and Powder River Pass dykes is the De Pass region of the Owl Creek Mountains, where a similarly orientated and faulted large dyke intrusion cuts through a small window of the basement (Thaden 1980). This mafic intrusion may be an outcrop of the same dyke (or network of dextrally offset dykes) as the South Pass and Powder River Pass dykes; however, no samples were collected from that locality.

Table 4. *Results from palaeomagnetic sites before and after tilt corrections*

			Site latitude (N)		Site longitude (W)		Before correction							After correction				
Site ID	Width (m)	Trend (deg)	(deg)	(min)	(deg)	(min)	Dec. (deg)	Inc. (deg)	a_{95} (deg)	Plat (°N)	Plong (°E)	a_{95} (deg)	$n(p)/N$	Dec. (deg)	Inc. (deg)	Plat (°N)	Plong (°E)	a_{95} (deg)
BH13	7.5	50	44	14.720	106	56.371	222.9	−66.1	2.4	60.5	319.5	3.5	8/8	–	–	–	–	–
BH14	40	15	44	20.752	106	53.721	122.7	−58.3	4	47.7	176.6	5	8/8	136.9	−64.8	60.1	183.2	5.7
BH15	40	50	44	14.380	106	55.945	209.4	−70.5	7.2	68.4	303.6	11.5	5/8	–	–	–	–	–
BH16	2.9	50	44	14.743	106	56.376	207.8	−61.2	7.7	69.8	338.9	10.4	6/7	–	–	–	–	–
BH17	4.8	55	44	14.802	106	56.368	228.9	−64.4	2.7	56.1	322.1	3.8	8/8	–	–	–	–	–
BH18	6.7	25	44	16.133	106	56.920	201.3	−62	11.5	74.6	339.4	15.8	4(1)/7	–	–	–	–	–
BH21	6.7	35	44	16.104	106	57.202	210.4	−67.9	3.4	68.6	314.1	5.3	8/8	–	–	–	–	–
BH22	>100	40	44	9.019	107	3.522	232.8	−48.2	3.3	45.9	344.4	3.5	8/8	–	–	–	–	–
BH24	50	20	44	4.182	106	59.978	141.4	−61.1	9.8	62.0	172.8	13.2	4(1)/8	123.1	−64.9	50.9	187.8	14.2
BH25	40	30	44	3.344	107	0.722	213.2	−41.4	14.8	56.2	8.8	14.1	4(2)/8	215.8	−51.1	59.5	354.5	16.5
BH58	13	58	44	15.616	106	51.600	177.1	−57.3	21.7	83.3	93.1	27.1	3(3)/8	191.6	−54.8	77.4	24.3	25.8
BH59	20	55	44	15.630	106	51.389	181.9	−46.4	4.6	73.4	67.3	4.8	7/8	191.5	−43.5	68.9	43.1	4.5
SHM3	70	45	44	11.464	107	0.343	239.5	−53.9	14.9	44.0	333.9	17.4	3(1)/8	–	–	–	–	–
QDmean*	>>100	10	42	26†	108	31†	354.9	64.6	4.6	84.6	211.2	6.6	8	36.9	59.7	62.5	332.8	6
WR-58a*	N/A	20	42	24.93	108	30.876	342.9	55.2	6.3	75.2	140.4	7.6	9(3)/10	22.7	51.8	69.5	3.1	7.1

Bold sites used for Rabbit Creek swarm mean calculation. α_{95}, 95 percent confidence interval; Dec., declination; Inc., inclination; Plat and Plong, palaeolatitude and palaeolongitude virtual geomagnetic pole coordinates, respectively; n, Number of samples (p, plane-fits) used in mean; N, number of samples collected and processed.
*Uses data from Harlan *et al.* (2003) with tilt correction of data about bedding first (323°/8° NE) then about a vertical axis (30° clockwise).
†See Harlan *et al.* (2003) for sampling locality information.

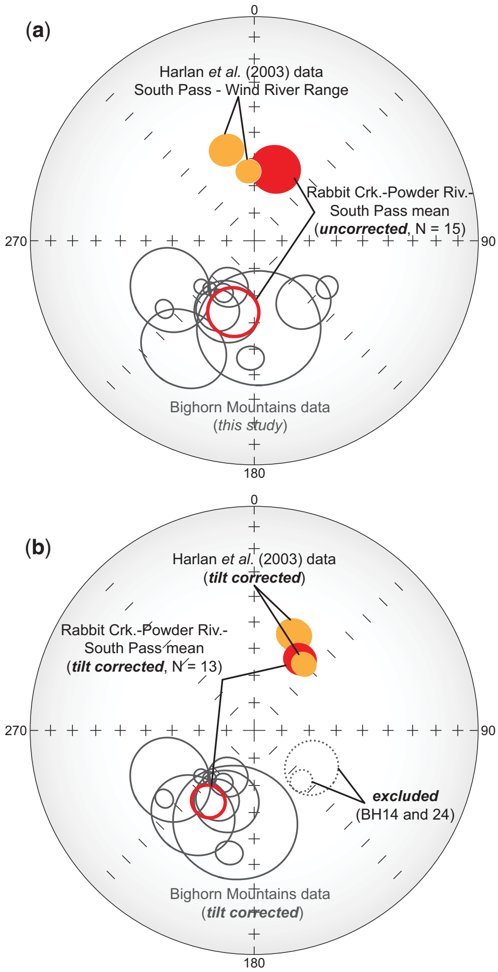

Fig. 7. Site mean data (local coordinates) for the Rabbit Creek swarm and Powder River Pass dykes (grey ellipses) along with data from South Pass dykes (orange ellipses) (Harlan *et al.* 2003) on equal-area plots. Filled ellipses indicate lower hemisphere directions (positive inclinations) whereas open ellipses indicate upper hemisphere directions (negative inclinations). (**a**) Before structural corrections are applied to data, the overall mean is composed of fairly scattered site means. All data are included in the Rabbit Creek–Powder River–South Pass uncorrected mean (red ellipse), also plotted in the lower hemisphere (open red ellipse). (**b**) Structurally corrected data in local coordinates with an improved Rabbit Creek–Powder River–South Pass mean (red ellipses). Sites BH14 and BH24 are judged as excursions and excluded from the mean calculation.

Because of the age difference between the Powder River–South Pass dykes (*c.* 2164 Ma) and the Rabbit Creek dykes (*c.* 2155 Ma), the palaeomagnetic data from Harlan *et al.* (2003) and the Powder River Pass dyke (BH22 and SHM3) are excluded from the Rabbit Creek palaeomagnetic pole (Table 6). In the case that all of the dykes in Bighorn Mountains represent a mixture of Rabbit Creek and Powder River dykes, we have also calculated an alternative palaeomagnetic pole for all Bighorn intrusions (excluding sites BH14 and BH24) that applies to a slightly longer time interval, 2171–2152 Ma. This age range is also assigned to the mean calculated for the South Pass–Powder River Pass and Rabbit Creek dykes. If South Pass data are corrected according to both horizontal and vertical-axis rotations (Table 4), the virtual geomagnetic poles agree very well with the Rabbit Creek pole (Fig. 7). The pole calculated from all corrected data from all ranges changes the mean coordinates by only a few degrees and reduces the error interval by less than a degree. Statistically, these three means are indistinct, possibly a result of under sampling the intrusions from the South Pass–Powder River Pass event (Table 6). We prefer to use the inclusive Rabbit Creek–Powder River–South Pass dykes palaeomagnetic pole (excluding BH14 and BH24) in our palaeogeographic analysis because it has the highest likelihood of fully averaging secular variation from 2171 to 2152 Ma.

Discussion

The 2171–2152 Ma event is well suited to palaeogeographic reconstructions with a positive baked-contact test, increased precision after tilt corrections and multiple high-precision U–Pb ages. However, subtle differences in some results within the swarm prompt questions about the spatial and temporal extent of the Rabbit Creek event and its relationship to the Powder River–South Pass dykes.

The Rabbit Creek swarm most likely intruded in less than 10 myr in the Bighorn Mountains but possibly in different generations (or pulses) of magmatism that are difficult to distinguish with geochronology because Rabbit Creek ages all overlap within uncertainty. Slight variations in trends among dykes are probably the result of the older shear fabric in the central and southern gneiss terrain (Frost & Fanning 2006) and are not reflected in geochemical and palaeomagnetic variations in the Bighorn Mountains. Dykes BH14 and BH24 have similar trends (010° and 015°, respectively), age and palaeomagnetic directions, but they are different geochemically. It appears that trend does not necessarily have a correlation with geochemistry, considering that dykes BH58 and BH59 have trends (050°) very different from BH24 (010°), but share similar major element, REE and Nd isotopic characteristics. Sites BH14, BH58 and BH59 are the closest localities to the edge of the uplift;

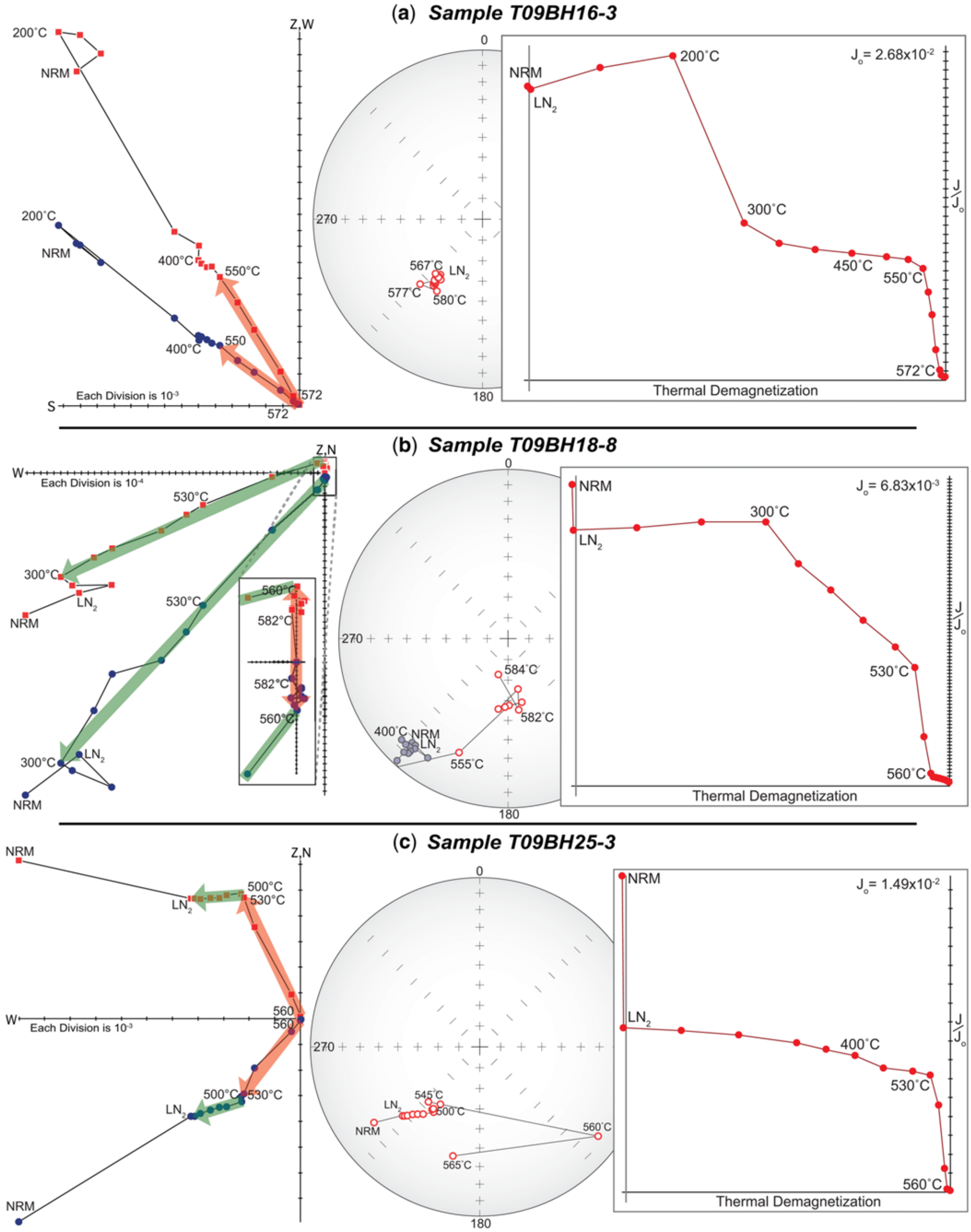

Fig. 8. The Rabbit Creek dyke's demagnetization behaviour is exemplified by samples from three different dykes. Each panel (a–c) displays measurements for the same samples on different diagrams (from left to right): orthogonal plot, equal-area plot, and J/J_0 intensity diagrams. Natural remanent magnetization indicates the initial measurement before any demagnetization, LN_2 indicates the measurement taken after liquid nitrogen immersion and subsequent labels indicate the temperature step of thermal demagnetization. J_0 is the initial intensity of the sample magnetization. Open red circles on the equal-area plots indicate negative inclinations and blue symbols indicate positive inclinations. On the orthogonal plot, red squares indicate inclination direction and blue circles represent declination. Orange vectors represent the least-squares fit of the primary magnetizations, whereas green vectors represent spurious magnetizations removed during the earlier stages of demagnetization. The lower-temperature components (green vectors) have similar directions in (b) and (c) but are not consistent enough in either dyke (or the region) to be of statistical significance.

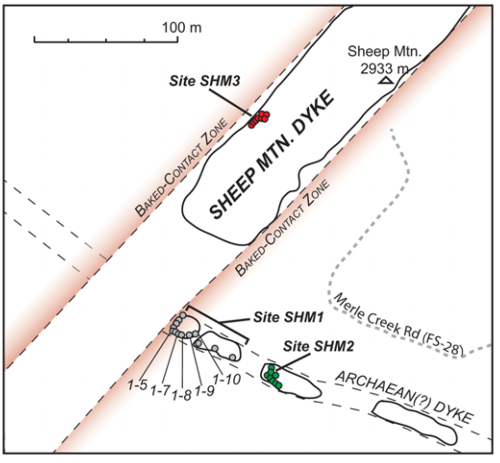

Fig. 9. Map of the Sheep Mountain dyke intersection with an Archaean(?) dyke; palaeomagnetic sampling sites are indicated. Surface exposures of the dykes are shown by solid black line polygons; dashed black lines indicate the inferred extent of intrusions. Sites in red indicate the locality where the Sheep Mountain dyke was sampled (SHM3), green sites identify the unbaked sample locality for the Archaean dyke and grey sites indicate the baked-contact test samples for the Sheep Mountain dyke. A baked-contact zone is shown as a red gradient, which is estimated from the demagnetization components isolated in samples SHM1-7, SHM1-8, SHM1-9 and similar to length scales of half-space cooling models proposed in Delaney (1987).

nonetheless it is very unlikely that structural rotations explain the discrepancies in trend and palaeomagnetism. Sites BH24 and BH25 are very near to each other geographically (1.8 km) and have similar REE concentrations, yet they have different trends (015° and 030°) and palaeomagnetic directions, suggesting that geochemical differences are most strongly correlated with the location of a dyke within the swarm. Sites BH24, BH25, BH58 and BH59 are the farthest SE localities sampled within the Bighorn Mountains and group well geochemically, distinct from all other sites from the northwestern dyke set. The lower MgO and incompatible element abundances in the southeastern group, low Th/La and higher Nd isotope ratios, are consistent with them representing a mantle-derived magma that has undergone some fractional crystallization with minimal crustal contamination.

The northwestern group may be related to the southeastern dyke magmas by a combination of fractional crystallization and crustal assimilation, based on the roughly parallel incompatible element patterns but lower MgO, higher Th/La and lower ε_{Nd} in the northwestern dykes. The range of compositions exhibited by the northwestern dyke set is not geographically controlled: BH17 and BH22 are very alike geochemically but are widely spaced, and adjacent samples BH13, BH16 and BH17 span the entire range of northwestern dyke compositions. The overlap in U–Pb ages between the two dyke groups indicates that all of these magmas were available to be emplaced throughout the history of the dyke swarm. The petrological variations over this time period are consistent with existence of a zoned magma reservoir feeding the swarm. The southeastern group magmas were derived either from the less differentiated core of the reservoir or from dyke-fed magmas that missed the reservoir and proceeded directly to the surface. The northwestern dykes tapped more fractionated and contaminated magmas from the margins of the reservoir.

The orientation of dykes within the Rabbit Creek swarm varies by *c.* 40° (010–050°), but there is not much evidence to support a correlation between trend and palaeomagnetic direction. As mentioned, the only sites that support a trend v. palaeomagnetic correlation are BH14 and BH24. Other intrusions often change their orientations along the length of the intrusion; for example, site BH11 was sampled in a dyke that appears to bifurcate, or change trends drastically over a short distance (Fig. 1). The dykes in this swarm may have simultaneously intruded in multiple orientations during the entire magmatic event, implying that, even if there were discrete sub-swarms over a 15 myr interval, they may not be easily defined by their orientations (i.e. there could have been a rapidly changing stress field). It is most likely that antecedent faults and structures in the basement gneiss of the southern Bighorns may relate to preferences in trend. Most of the river valleys in the SE Bighorn region are controlled by large, NE-trending faults that extend for tens of kilometres. The faults often contain mylonitic zones with foliation and coplanar cleavage, parallel to the fault orientations. These roughly NE-trending faults cross-cut Archaean dykes and have identical variations in orientation (010–050°) to the Rabbit Creek dykes, intimating that the swarm preferentially intruded along these faults with offshoots of slightly different trends. Faults with more northerly orientations (010°) are mapped in the vicinity of both BH14 and BH24, and they possibly served as pre-existing fractures that allowed dykes to jog or jump before continuing along the dominant NE fault plane orientations. A later generation of ESE-trending faults offset some Rabbit Creek dykes, but their minimum age is unknown and they may be related to the Trans-Hudson Orogeny, the Laramide Orogeny, or anything in between.

Great Dyke of Wyoming?

The large (>100 m-wide) dykes that crop out in the southern Bighorn Mountains (Powder River Pass

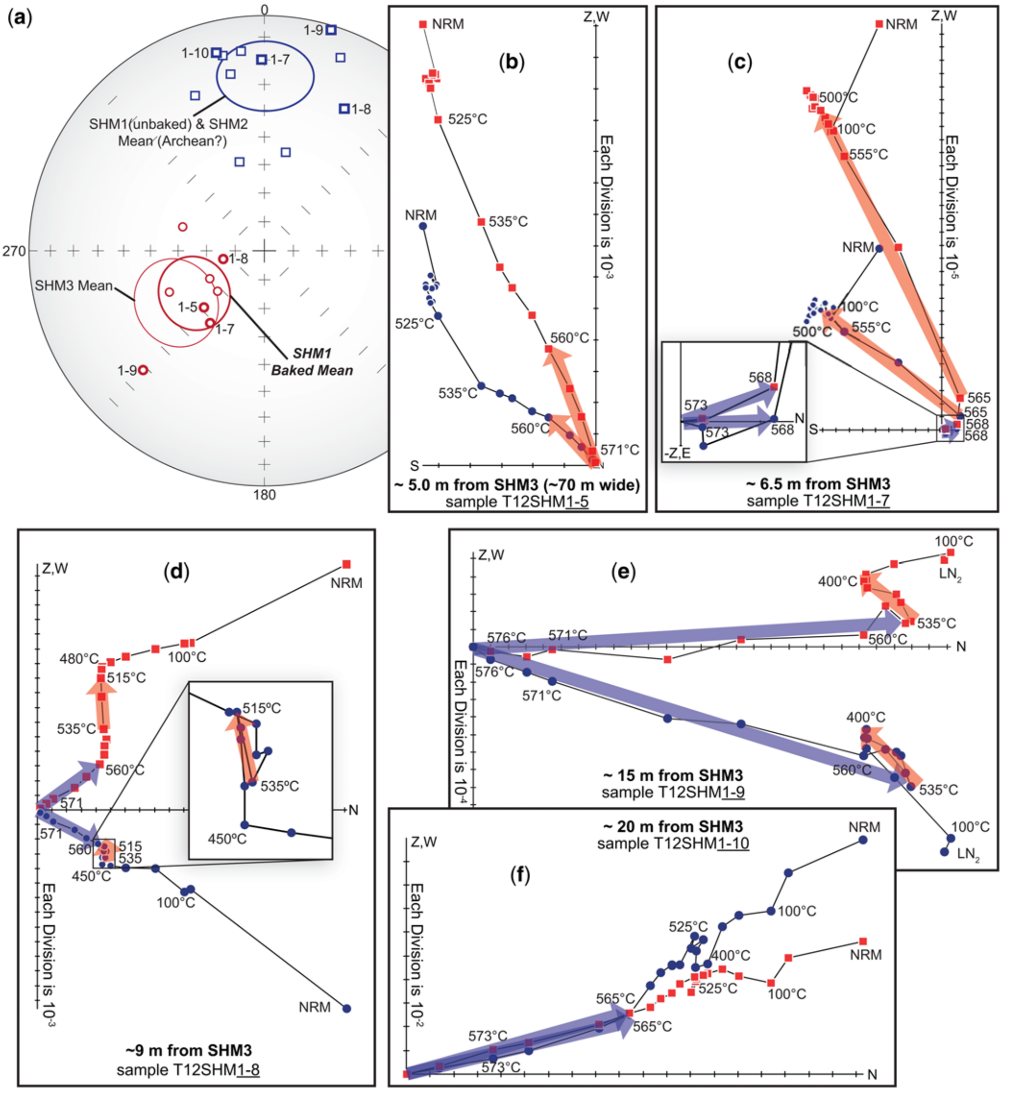

Fig. 10. Data from the baked-contact test for the Sheep Mountain dyke (SHM3) showing (**a**) an equal-area plot with all magnetization components isolated from SHM1, SHM2 and SHM3, excluding a small number of samples that were probably struck by lightning. Red circles indicate baked components and blue squares indicate unbaked components (from SHM1 and SHM2). Site means are shown for the unbaked direction (SHM1 and SHM2), the intruding Sheep Mountain dyke (SHM3) and baked components from SHM1 samples close to the intrusion. Sample directions with bold symbols correspond to the vectors shown in (b–f). (**b**) Sample SHM1-5 is shown in an orthogonal plot to be completely baked by the Sheep Mountain dyke at *c.* 5 m away. Remanence removed at lower temperatures is only slightly different than the baked direction, with blue circles (red squares) representing declination (inclination) data. (**c**) Demagnetization data from hybrid sample SHM1-7 shown in an orthogonal plot. Orange vectors indicate the lower-temperature baked magnetization and blue vectors indicate the high-temperature unbaked remanence direction from grains not heated long enough to reset their magnetization. (**d**) An orthogonal plot for sample SHM1-8 shows the progression of the hybrid zone away from the intruding dyke, with a baked component that is removed at *c.* 535 °C. (**e**) An orthogonal plot for sample SHM1-9 showing a small baked component up to 530 °C, with an unbaked component at high temperatures that dominated the sample magnetization. (**f**) An orthogonal plot of sample SHM1-10, which has no perceivable baked component and a very strong unbaked magnetization. The decrease in magnitude of the baked component (orange vectors) and increase in unbaked remanence magnitude (blue vectors) correspond to the dissipation of a partial TRM with increasing distance from the heat source (Sheep Mountain dyke). In both (c) and (d) certain areas of the plot have been magnified to better display magnetic components.

Table 5. *Tilt-correction parameters for each palaeomagnetic site*

Site ID	Nearby bedding attitude (RHD) Strike	Dip	Tilt correction reference
BH24	110	10	Hoppin *et al.* (1965)
BH14	350	10	Hoppin *et al.* (1965)
BH25	110	10	Hoppin *et al.* (1965)
BH22	*No significant correction*		Hoy & Ridgway (1997)
BH18	*No significant correction*		Hoy & Ridgway (1997)
BH16	*No significant correction*		Hoy & Ridgway (1997)
BH21	*No significant correction*		Hoy & Ridgway (1997)
BH15	*No significant correction*		Hoy & Ridgway (1997)
BH13	*No significant correction*		Hoy & Ridgway (1997)
BH17	*No significant correction*		Hoy & Ridgway (1997)
BH58	350	10	Hoy & Ridgway (1997)
BH59	350	10	Hoy & Ridgway (1997)
SHM3	*No significant correction*		Hoy & Ridgway (1997)
Qdmean*	323	8	Hausel (1988)
WR-58a*	323	8	Hausel (1988)

References indicate the source of bedding data or estimations. RHD refers to the dip direction, which is 90° clockwise from the strike direction.
*Requires an additional vertical-axis correction; see Table 4 and text.

dyke, sites BH22, BH26 and SHM3) and in South Pass (the dyke of Harlan *et al.* (2003), and sample BNB-09-WY-210b) are very probably the same intrusion that spans more than 200 km in length. There are many distinct characteristics linking these intrusions to each other. For instance, both dykes are unique in their large size and reach over 100 m width at both localities. They each show 10–15 m of inward-coarsening diabase on either margin within single outcrops, with a narrow transition to a leucogabbro (to quartz–diorite) core. In the Bighorn Mountains, South Pass and Owl Creek Mountains, large offshoot dykes of diabase surround each intrusion, with orientations 10–20° clockwise from the main intrusions and right-stepping en echelon offsets along their lengths. The features of these intrusions are unique within the Wyoming craton, providing a strong geological correlation supported by indistinguishable U–Pb ages. If faults in the South Pass region are restored and the SE region of the Wind River uplift is corrected for a vertical-axis rotation, then outcrops of the hypothesized Great Dyke of Wyoming appear nearly along the same NE-trending line (Fig. 11).

Additional supporting evidence for the existence of a continuous 'Great Dyke of Wyoming' is the presence of a similarly large intrusive body mapped in the eastern Owl Creek Mountains (Thaden 1980). This dyke appears almost directly between the two other outcrops in the Bighorn Mountains and Wind River Range, but it is oriented more northerly. Such an orientation may be due to block rotations during the Laramide Orogeny, when major faulting and transport of nearby Palaeozoic rocks occurred, leaving fault gouges along some dyke margins. The orientations of the South Pass and De Pass dykes may be emblematic of one large intrusion that has a NNE-trend and right-stepping en echelon offsets along its length, giving an apparent NE-trend to the intrusion on a regional scale.

There is also a significant possibility that the Powder River Pass dyke and the South Pass dyke are from separate magmatic pulses. The lack of continuous outcrop and the intrinsic uncertainty in radiometric dating do not provide a strong enough basis to affirm that they are parts of the same intrusive body. The palaeomagnetic results highlight this ambiguity because they are of different magnetic polarities. Thermal and alternating field demagnetization results from the South Pass dyke (Harlan *et al.* 2003) have a positive inclination, whereas all results from the Bighorn Mountains (this study), including the wide Powder River Pass dyke (BH22 and SHM3), have negative inclinations. The positive baked-contact test confirms the primary nature of the negative inclination, while the results from South Pass are almost identical to the present local field direction (before tilt correction). Given this scenario, there are a few possible interpretations with varying amounts of likelihood. (1) Both palaeomagnetic results could be primary TRMs from the long-term cooling of one large intrusion (or distinct pulses into the same intrusion); a dyke of this size (>100 m) could take over 500 years to cool below

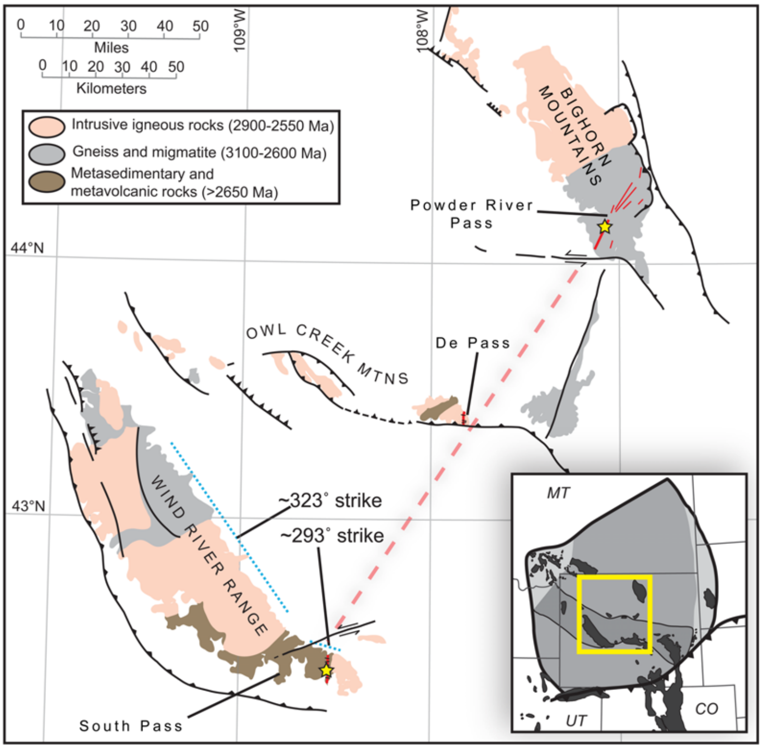

Fig. 11. Regional map showing Precambrian rocks of three Laramide uplifts. The inset map indicates the location of this figure on a larger scale. Yellow stars indicate the location of the Powder River Pass dyke in the Bighorn Mountains and the South Pass dyke in the Wind River Range. After correcting for the vertical-axis rotation of the southeastern limb of the Wind River uplift, outcrops of the intrusions appear to line up with each other from South Pass to the Bighorn Mountains (dashed red line is the inferred extent of the Great Dyke of Wyoming underneath Palaeozoic cover). The dashed red line may not resemble the actual igneous bodies, which may be a network of NNE-trending dykes that intruded with significant en echelon offsets along its length that were additionally displaced by later dextral faults. In between uplifts are deep Phanaerozoic basins that completely obscure the Precambrian basement rocks. The blue dashed lines indicate the approximate strike of the Wind River thrust that takes a 30° turn north of South Pass, which agrees with the attitude of Palaeozoic sediments along the northern side of the range and is the premise for needing an additional vertical-axis correction in the SE Wind River Range. Black lines indicate major faults with teeth indicating the hanging wall of thrust faults. Map modified from Sims *et al.* (2001).

300 °C at its centre (Delaney 1987). However, this is not likely because results were consistent across the width of each intrusion, where one might expect to see the effects of differential cooling rates. (2) Considering the time it took the large dyke to propagate over 200 km, both results could be primary TRMs with different ages. Again, this contingency is also unlikely given estimates of quite rapid dyke propagation over a period of days (Sigurdsson 1987; Keir *et al.* 2011). (3) The palaeomagnetic data from the South Pass dyke (Harlan *et al.* 2003) could be the result of deuteric oxidation of Fe–Ti oxides during the late stages of dyke cooling, which would still be considered a primary magnetization for the purposes of tectonic reconstructions. (4) The outcrops in the Bighorns and South Pass could expose different erosional levels of the dyke with either outcrop having come from a deeper region of the crust. In this scenario, crustal temperatures were higher at the time of intrusion and could have had a profound impact on when magnetite acquired its magnetization, possibly long after the intrusion of magma (Halls & Zhang 2003). (5) It is also possible that the positive inclination of the dyke is a VRM acquired more recently, though this is unlikely with the magnetization being held by magnetite up to the 570 °C and an $^{40}Ar/^{39}Ar$ amphibole age of 2124 ± 30 Ma determined by Harlan *et al.* (2003).

Palaeomagnetic results from the Powder River Pass dyke (BH22 and SHM3) and the two intrusions from South Pass (Harlan *et al.* 2003) are not enough to calculate a fully averaged palaeomagnetic

Table 6. *Palaeomagnetic poles from this study before and after structural corrections*

Palaeomagnetic pole	Age range (Ma)	Plat (°N)	Plong (°E)	a_{95}	*N*	*k*
Before corrections						
Rabbit Creek, Powder River and South Pass dykes (all sites)	2171–2152	78.4	332.0	13.1	15	9.5
Rabbit Creek, Powder River and South Pass dykes (except BH(14 and 24))	2171–2152	71.9	338.8	10.9	13	15.5
Rabbit Creek dykes (except SHM3 and BH(14, 22 and 24))	2161–2152	72.0	338.5	10.6	9	24.3
After corrections						
Rabbit Creek, Powder River and South Pass dykes (all sites)	2171–2152	72.1	332.3	11.8	15	11.5
Rabbit Creek, Powder River and South Pass dykes (except BH(14 and 24))	2171–2152	65.5	339.2	7.6	13	30.5
Rabbit Creek and Powder River dykes (except BH(14 and 24))	2171–2152	65.2	338.0	9	11	26.6
Rabbit Creek dykes (except SHM3 and BH(14, 22 and 24))	2161–2152	69.7	337.5	8.7	9	36

pole. After tilt correction the VGPs are fairly close to each other and not significantly different from Rabbit Creek dyke data, but because they may be the only cooling units of that age, it is statistically problematic to contrast them to the Rabbit Creek data.

The northern extent of the Powder River Pass dyke is hard to follow in the field and on satellite imagery. Northeast of site BH22 the dyke appears to bifurcate, as a portion continues north while another branch continues through Sheep Mountain (Fig. 1). The dyke then becomes thinner and less prominent topographically as it is offset by multiple, small sinistral faults. As it is about to cross Route 16 (NE of site BH15), the small ridge (presumed to be the intrusion) disappears into a river drainage. At first, there was concern that the northeastern extent of the Sheep Mountain (Powder River Pass) dyke may be related to dykes BH13, BH16 and BH17, offset along a sinistral fault that clearly cuts the nearby Rabbit Creek dyke. However, the displacement of the fault can clearly be measured using the Rabbit Creek dyke, which is offset by *c.* 100 m. The fault would have to offset the Powder River Pass dyke over 400 m to align with BH13, which is *c.* 7.5 m wide and very fine-grained. We conclude that the Powder River Pass dyke ends somewhere in the wetlands between sites BH15 and BH13, shrinking to such a small size that it is impossible to follow.

The intrusions we suspect to be parts of the 'Great Dyke of Wyoming' are distinct from a magnetic anomaly to the east of the Bighorn Mountains that was called by the same name (Gay 2003). That subsurface body is tens of kilometres wide and is interpreted by others as an Archaean domain boundary (Sims *et al.* 2001), but its affinity and composition remain unknown.

Global age comparisons

The Rabbit Creek event has few direct age matches with known events in other cratons. The South Pass dyke was previously assigned a slightly older age of 2170 ± 8 Ma, the result of U–Pb analyses with 20–30% discordance (Harlan *et al.* 2003). Our new dates for the South Pass–Powder River event permit a correlation with the Biscotasing event of southern Superior, which has an age span obtained from multiple dykes of 2165–2176 Ma (Halls & Davis 2004), within error of both Harlan *et al.* (2003) and our age estimates, yet distinct from the younger Rabbit Creek intrusions (202b, 204 and 207b). Neither of these new ages support a plausible correlation to the SW Slave Magmatic Province of the Slave craton, which has an older age range of 2175–2193 Ma (Bleeker & Hall 2007).

Globally, the *c.* 2155 Ma magmatic age is relatively rare. One of the few magmatic events that is nearly coeval is the Rivière du Gué swarm in northeastern Superior, dated at 2149 ± 3 Ma (Maurice *et al.* 2009). If Wyoming is reconstructed to southern Superior, as in Roscoe & Card (1993), then the Rabbit Creek and Rivière du Gué swarms could be distally related to the same event. Other near age matches include the Avayalik dykes of the North Atlantic craton (Nain portion) at 2142 ± 2 Ma (Connelly 2001), and the Hengling swarm of the North China craton at 2147 ± 5 Ma (Peng *et al.* 2005). Both of these events are slightly younger than the Rabbit Creek swarm and currently have no palaeomagnetic data available for comparison.

Palaeogeography

The Superior craton has a palaeomagnetic dataset that spans the time interval of the Rabbit Creek swarm, providing a convenient test for the Roscoe & Card (1993) fit of SE Wyoming against southern Superior. The Biscotasing swarm (Buchan *et al.* 1993) and the Marathon swarm (normal polarity) at 2126–2121 Ma (Buchan *et al.* 1993; Halls *et al.* 2005) both have reliable palaeomagnetic data supported by field tests. Because the Wyoming craton has no other Rhyacian (2300–2050 Ma) palaeomagnetic data, there is complete freedom of Wyoming's position in palaeolongitude.

The Marathon dyke swarm was emplaced on the southern margin of the Superior craton in two discernable pulses, 2101–2106 and 2121–2126 Ma (Hamilton *et al.* 2002), both postdating the Rabbit Creek swarm. The Biscotasing swarm is slightly older, at 2165–2176 Ma, and has large dykes that extend from southern Superior to the NE portion of the craton, where the centre of the event is hypothesized to exist with additional coeval dyke swarms and sills (Ernst & Bleeker 2010). Although neither of these events matches the Rabbit Creek swarm in age, they define an apparent polar wander path segment that includes the age of the Rabbit Creek swarm for comparison (Fig. 12). The Biscotasing swarm age roughly agrees with ages from the South Pass and Powder River Pass dykes at *c.* 2164 Ma, suggesting that both swarms intruded during the same event while Superior and Wyoming were connected. However, it is unknown how many other dykes in Wyoming belong to the slightly older 2164 Ma group, limiting a palaeomagnetic comparison.

We reconstructed Wyoming against Superior by placing the Huronian and Snowy Pass Supergroups in close proximity, according to the correlations of Roscoe & Card (1993), and then rotated Wyoming counter-clockwise until the Rabbit Creek pole intersected with the Superior apparent polar wander path (Fig. 12). The structurally corrected palaeomagnetic pole of the Rabbit Creek–Powder River–South Pass dykes (65.5°N, 339.2°E, $a_{95} = 7.6°$) reconstructs very well to the correct age range between the Biscotasing and Marathon swarm poles from Superior, with enough leeway to reconstruct Wyoming anywhere along southwestern Superior. Unfortunately, with only one palaeomagnetic pole for comparison, Wyoming's relative position cannot be pinpointed (it is only possible to know its palaeolatitude) and could instead lie anywhere along the dashed grey small circle in Figure 12. Nevertheless, it is remarkable that the palaeomagnetic data allow a precise connection between two Palaeoproterozoic sedimentary sequences predicted as proximally related to an early Proterozoic aulacogen (Karlstrom *et al.* 1983), as shown in our reconstruction.

The two dykes BH14 (202b) and BH24 (207b) are quite distinct geochemically but they are both closely related in age, 2155.9 ± 2.9 and 2157.7 ± 3.6 Ma, and yield similar irregular palaeomagnetic directions. These anomalous magnetizations are excluded in calculating a palaeomagnetic pole, but when reconstructed using the fit provided herein, they fall beyond the Biscotasing pole from the Superior craton (Fig. 12). These unexpected directions are probably due to a short-lived magnetic excursion caused by relatively stronger non-dipole components (i.e. quadrupole and octupole), possibly owing to a drop in intensity of the geocentric axial dipole (Roberts 2008). This could be evaluated by conducting palaeointensity experiments to see if the geomagnetic field was weaker during the intrusion of BH14 and BH24. It is unlikely that this excursion can be explained by a true polar wander event, such as those known to occur later in this era (Mitchell *et al.* 2010), because rates would probably exceed the maximum allowed, even for fast rate estimates for true polar wander (Tsai & Stevenson 2007).

Wyoming and Superior are only two Archaean fragments of many, so it is difficult to make a conclusive case for the existence of either supercontinent Kenorland (Williams *et al.* 1991) or supercraton Superia (Bleeker 2003) based on this one reconstruction; the Superior–Wyoming landmass could have been part of either. However, the configuration presented in this study fits the model for supercraton Superia described by Ernst & Bleeker (2010), which includes the correlations of the Karelia, Kola and Hearne cratons (Bleeker & Ernst 2006) based upon coeval magmatic events at *c.* 2210, 2110 and 2000 Ma. The reconstruction calculated in this study refines the possible fit of Wyoming to southern Superior (Euler pole: 48°N, 265°E, +125° CCW), juxtaposing the Snowy Pass and Huronian Supergroups along with a number of mafic magmatic events temporally close to the Rabbit Creek swarm. Magmatism was concentrated in southern Superior for 100 myr, from the *c.* 2170 Biscotasing dykes until the *c.* 2070 Ma Fort Frances dykes. Magmatism in Wyoming occurs over nearly the same interval, from 2165 to 2010 Ma, but no ages in southern Superior match with the Rabbit Creek swarm. One of the many dykes that remain undated in southern Superior may provide a link to Rabbit Creek magmatism in Wyoming.

A failed rift basin that formed between Superior and Wyoming during the Matachewan event

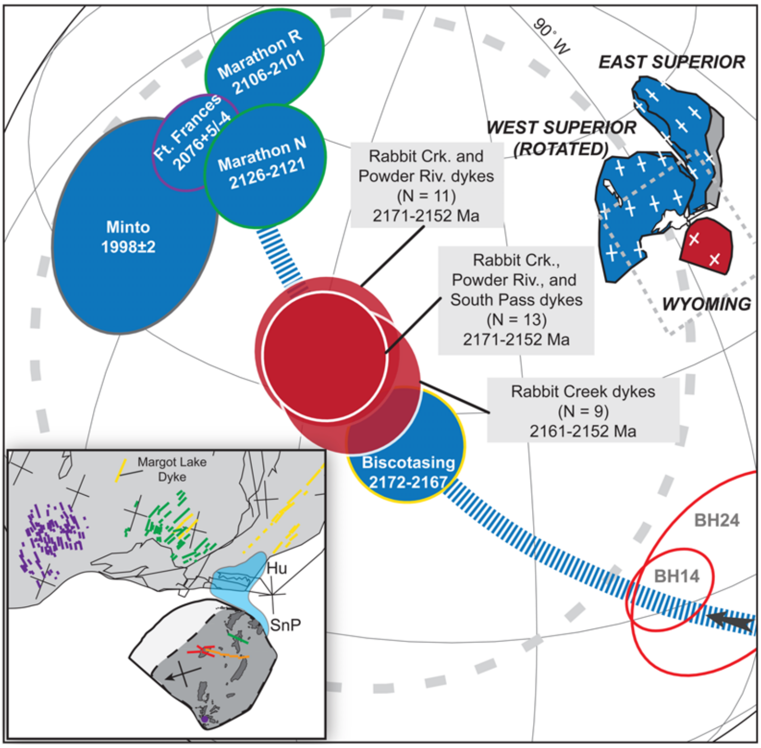

Fig. 12. Reconstruction of the Wyoming craton to the Superior craton at *c*. 2160 Ma. Palaeomagnetic poles for Superior are filled with blue, and Wyoming and its poles are coloured red. The Rabbit Creek–Powder River–South Pass pole is displayed with two other poles (opaque red ellipses) calculated for Wyoming, one using solely the Rabbit Creek data, another excluding South Pass dyke data. The eastern Superior craton has present day coordinates with western Superior rotated, accounting for late Palaeoproterozoic Kapuskasing Zone deformation (Bates & Halls 1991; Evans & Halls 2010). The applied Euler rotation (Wyoming to eastern Superior; 48°N, 265°E, 125°CCW) brings the 2171 to 2152 Ma pole in between data from the Biscotasing and Marathon swarms along the Superior apparent polar wander path (dashed blue curve), which extends back in time towards the *c*. 2215 Ma Nipissing palaeomagnetic pole (not visible in figure). There is complete freedom for Wyoming to rotate in palaeolongitude (i.e. in space about the Rabbit Creek pole), with possible locations defining the grey small circle centred on the Rabbit Creek pole, but the preferred reconstruction also aligns the Snowy Pass and Huronian Supergroups (basins shown as connected in light blue; after Roscoe & Card (1993)). There is also enough flexibility in the palaeomagnetic fit to move Wyoming slightly to the east while maintaining the stratigraphic correlation. The two magnetic excursion results (BH14 and BH24) are shown in the bottom right (open red ellipses), falling earlier along Superior's apparent polar wander path. The inset shows a magnified view of the Superior–Wyoming boundary in this proposed fit. Relevant dyke swarms are in various colours (red, Rabbit Creek swarm; yellow, Biscotasing swarm; green, Marathon swarm and the Bear Mountain dyke of Wyoming (Bowers & Chamberlain 2006); purple, Fort Frances swarm and metamorphosed intrusions of Wyoming (Mueller *et al*. 2004); and orange, Powder River–South Pass dykes). These dyke swarms all fall along a possible long-lived rift zone, with colours of dyke swarms corresponding to the outlines of palaeomagnetic poles. West Superior and its palaeomagnetic data have been rotated according to Evans & Halls (2010).

(Heaman 1997) could have persisted through the Palaeoproterozoic, finally becoming a successful rift sometime between 2100 and 2000 Ma. Stratigraphic correlations (Bekker *et al.* 2005) matching southeastern Wyoming to southern Superior and other possible cratons support this prospect. Karelia has multiple large mafic events with broad age ranges that fit well with Wyoming/Superior, at *c*. 2000, 2110 and 2210 Ma (Vuollo & Huhma 2005), leading some to reconstruct it next to both Wyoming and Superior during this time (Bleeker 2003; Ernst & Bleeker 2010). The Hearne craton contains the Griffin gabbros at *c*. 2110 Ma (Heaman & LeCheminant 1993; Aspler *et al.* 2002), a magmatic age found on all cratons mentioned. This could be an indication that Wyoming, Superior, Karelia and Hearne were all part of the same large rifting event, maybe even involving Nain, where a diabase dyke has an age of 2121 ± 1.5 Ma (Hamilton *et al.* 1998).

Conclusion

The Rabbit Creek swarm provides new palaeomagnetic and geochemical data during a key interval in Earth history. The Wyoming–Superior link is possible, if not probable additional palaeomagnetic results from already dated mafic dyke swarms will be useful to test synchronous motion of the Wyoming–Superior (Superia?) landmass. The Rabbit Creek event has no direct age matches with other blocks, but it occurs during an interval of frequent and voluminous magmatism over much of the southern Superior craton. In our reconstruction of Wyoming (Fig. 12), the Rabbit Creek dykes do not point directly north towards the margin of Superior and are therefore not expected to continue into the adjacent craton. However, the Rabbit Creek dykes do point towards a hypothesized plume or rift region (Halls *et al.* 2008) on the margin of Superior that occurs soon afterwards, defined by the radiating pattern of the Marathon and Fort Frances dykes (2125 and 2070 Ma). Our fit points the Bear Mountain dyke (*c.* 2110 Ma) in Wyoming towards the Marathon dykes in Superior and directly juxtaposes the Snowy Pass and Huronian Supergroups as part of a single basin, possibly an aulacogen from early Palaeoproterozoic rifting that was reactivated during the late Palaeoproterozoic (Karlstrom *et al.* 1983). The Powder River–South Pass dykes overlap in age with the Biscotasing swarm, but they do not line up along-strike in our reconstruction (Fig. 12). This could be the result of the stress field that existed during the intrusion of these dykes, defining the orientations at which fractures formed and propagated. Stress fields are broadly consistent on continental scales but can curve significantly near and across major tectonic structures, accounting for differences in trend between dyke swarms on separate yet adjacent cratons.

The Powder River–South Pass dykes could also be related to coincidental magmatism on another adjacent block or perhaps to another centre of magmatism on SW Superior related to the Biscotasing dykes (Dahl *et al.* 2006). The latter is supported by a U–Pb age from the NNE-trending Margot Lake dyke in central Superior (Fig. 12) at 2174.6 ± 3.2 Ma (Hamilton & Stott 2008), which has a significantly different trend from the Biscotasing dykes even after correcting for late Palaeoproterozoic rotation between east and west Superior (Evans & Halls 2010). Like the Rabbit Creek dyke magnetization, the Margot Lake dyke is of purportedly 'reversed' magnetic polarity (Hamilton & Stott 2008), whereas the rest of the Biscotasing swarm is of 'normal' polarity (lower hemisphere directions). This array of *c.* 2170 Ma dyke trends produces a piercing point on the southern margin of Superior, far different from another possible piercing point in northwestern Superior defined by the Biscotasing dykes, Labrador trough magmatism (Rohon *et al.* 1993) and Payne River dykes (Ernst & Bleeker 2010).

Previously, it was unknown whether thrusting during the Laramide Orogeny resulted in vertical-axis rotations of regional-scale basement blocks, making a craton-wide reference frame intractable. Our results suggest that the cores of Precambrian uplifts are buttressed by the craton in the subsurface, requiring only small tilt corrections. Rotated basement blocks on the margins of uplifts (e.g. the South Pass region) are more susceptible to vertical and horizontal rotations but could be recoverable after structural restorations (Fig. 7). Though a more comprehensive statistical comparison is necessary between exposures of the Wyoming craton, by establishing the first primary palaeomagnetic pole for this time interval, our results create a robust Proterozoic reference frame for the core of the Wyoming craton in the Bighorn uplift. In addition, we put forth strong evidence for the 'Great Dyke of Wyoming', which spans almost half of the Wyoming craton.

Financial support for part of this work was provided by NSF grants EAR-1019739 (palaeomagnetic work, at Yale) and collaborative NSF grant EAR-1019595 (geochronological work, at University of Wyoming). This is publication no. 40 of the Large Igneous Provinces – Supercontinent Reconstruction, Industry–Government–Academia Consortium Project (www.supercontinent.org; NSERC CRDPJ 419503-11; CAMIRO Project 08E03). We thank R. Mitchell, R. Ernst, J. Panzik and A. LeCheminant for insightful discussions and assistance with fieldwork, and also H. Halls and an anonymous reviewer for helping to greatly improve this manuscript.

References

Ansdell, K. M. & Heaman, L. M. *et al.* 2005. Correlation chart of the evolution of the trans-Hudson orogen–Manitoba–Saskatchewan segment. *Canadian Journal of Earth Sciences*, **42**, 761, http://doi.org/10.1139/e05-004

Aspler, L. B. & Chiarenzelli, J. R. 1998. Two Neoarchean supercontinents? Evidence from the Paleoproterozoic. *Sedimentary Geology*, **120**, 75–104.

Aspler, L. B., Cousens, B. L. & Chiarenzelli, J. R. 2002. Griffin gabbro sills (2.11 Ga), Hurwitz Basin, Nunavut, Canada: long-distance lateral transport of magmas in western Churchill Province crust. *Precambrian Research*, **117**, 269–294, http://doi.org/10.1016/S0301-9268(02)00090-6

Barnhart, K. R., Mahan, K. H., Blackburn, T. J., Bowring, S. A. & Dudas, F. O. 2012. Deep crustal xenoliths from central Montana, USA: implications for the timing and mechanisms of high-velocity lower crust formation. *Geosphere*, **8**, 1408–1428, http://doi.org/10.1130/ges00765.1

Bates, M. P. & Halls, H. C. 1991. Broad-scale Proterozoic deformation of the central Superior Province revealed by paleomagnetism of the 2.45 Ga Matachewan dyke swarm. *Canadian Journal of Earth Sciences*, **28**, 1780–1796, http://doi.org/10.1139/e91-159

Bekker, A. & Eriksson, K. A. 2003. A Paleoproterozoic drowned carbonate platform on the southeastern margin of the Wyoming Craton: a record of the Kenorland breakup. *Precambrian Research*, **120**, 327–364, http://doi.org/10.1016/s0301-9268(02)00165-1

Bekker, A., Kaufman, A. J., Karhu, J. A. & Eriksson, K. A. 2005. Evidence for Paleoproterozoic cap carbonates in North America. *Precambrian Research*, **137**, 167–206, http://doi.org/10.1016/j.precamres.2005.03.009

Blackwelder, E. 1926. Pre-Cambrian geology of the Medicine Bow Mountains. *Geological Society of America Bulletin*, **37**, 615–658.

Bleeker, W. 2003. The late Archean record: a puzzle in *c.* 35 pieces. *Lithos*, **71**, 99–134.

Bleeker, W. & Ernst, R. 2006. Short-lived mantle generated magmatic events and their dyke swarms: the key to unlocking Earth's paleogeographic record back to 2.6 Ga. *In*: Hanski, E., Mertanen, S., Rämö, T. & Vuollo, J. (eds) *Dyke Swarms—Time Markers of Crustal Evolution*. Taylor & Francis, London, 3–26.

Bleeker, W. & Hall, B. 2007. The Slave Craton: geology and metallogenic evolution. *In*: Goodfellow, W. D. (ed.) *Mineral Deposits of Canada: A Synthesis of Major Deposit-Types, District Metallogeny, the Evolution of Geological Provinces, and Exploration Methods*. Geological Association of Canada, Mineral Deposits Division, Special Publications, **5**, 849–879.

Bowers, N. E. & Chamberlain, K. R. 2006. Precambrian history of the eastern Ferris mountains and Bear mountain, south-central Wyoming Province. *Canadian Journal of Earth Sciences*, **43**, 1467–1487.

Brady, J. B., Mohlman, H. K., Harris, C., Carmichael, S. K., Jacob, L. J. & Chaparro, W. R. 2004. *General Geology and Geochemistry of Metamorphosed Proterozoic Mafic Dikes and Sills, Tobacco Root Mountains, Montana*. Geological Society of America, Boulder, CO, Special Papers, **377**, 89–104, http://doi.org/10.1130/0-8137-2377-9.89

Brown, W. G. 1993. Structural style of Laramide basement-cored uplifts and associated folds. *Geology of Wyoming: Geological Survey of Wyoming Memoir*, **5**, 312–371.

Buchan, K. L. 1991. Baked contact test demonstrates primary nature of dominant (N1) magnetisation of Nipissing intrusions in Southern Province, Canadian Shield. *Earth and Planetary Science Letters*, **105**, 492–499.

Buchan, K. L., Mortensen, J. K. & Card, K. D. 1993. Northeast-trending Early Proterozoic dykes of southern Superior Province: multiple episodes of emplacement recognized from integrated paleomagnetism and U–Pb geochronology. *Canadian Journal of Earth Sciences*, **30**, 1286–1296.

Buchan, K. L., Halls, H. C. & Mortensen, J. K. 1996. Paleomagnetism, U–Pb geochronology, and geochemistry of Marathon dykes, Superior Province, and comparison with the Fort Frances swarm. *Canadian Journal of Earth Sciences*, **33**, 1583–1595.

Buchan, K. L., Mortensen, J. K., Card, K. D. & Percival, J. A. 1998. Paleomagnetism and U–Pb geochronology of diabase dyke swarms of Minto block, Superior Province, Quebec, Canada. *Canadian Journal of Earth Sciences*, **35**, 1054–1069.

Buchan, K. L., Mertanen, S., Park, R. G., Pesonen, L. J., Elming, S.Å., Abrahamsen, N. & Bylund, G. 2000. Comparing the drift of Laurentia and Baltica in the Proterozoic: the importance of key palaeomagnetic poles. *Tectonophysics*, **319**, 167–198.

Buchan, K. L., Goutier, J., Hamilton, M. A., Ernst, R. E. & Matthews, W. A. 2007. Paleomagnetism, U–Pb geochronology, and geochemistry of Lac Esprit and other dyke swarms, James Bay area, Quebec, and implications for Paleoproterozoic deformation of the Superior Province. *Canadian Journal of Earth Sciences*, **44**, 643–664.

Chamberlain, K. R. & Mueller, P. A. 2007. Chapter 6.3 oldest rocks of the Wyoming craton. *In*: Martin, J., van Kranendonk, R. H. S. & Vickie, C. B. (eds) *Developments in Precambrian Geology*. Elsevier, Oxford, 775–791.

Chamberlain, K. R., Frost, C. D. & Frost, B. R. 2003. Early Archean to mesoproterozoic evolution of the Wyoming province: Archean origins to modern lithospheric architecture. *Canadian Journal of Earth Sciences*, **40**, 1357–1374.

Cogné, J. P. 2003. PaleoMac: a Macintosh^{TM} application for treating paleomagnetic data and making plate reconstructions. *Geochemistry, Geophysics, Geosystems*, **4**, 1007–1014, http://doi.org/10.1029/2001GC000227

Collinson, D. W. & Runcorn, S. K. 1960. Polar wandering and continental drift: evidence from paleomagnetic observations in the United States. *Geological Society of America Bulletin*, **71**, 915–958, http://doi.org/10.1130/0016-7606(1960)71[915:pwacde]2.0.co;2

Condie, K. C., Barsky, C. K. & Mueller, P. A. 1969. Geochemistry of precambrian diabase dikes from wyoming. *Geochimica et Cosmochimica Acta*, **33**, 1371–1388.

Connelly, J. N. 2001. Constraining the timing of metamorphism: U–Pb and Sm–Nd Ages from a transect across the Northern Torngat Orogen, Labrador, Canada. *The Journal of Geology*, **109**, 57–77, http://doi.org/10.1086/317965

Cousens, B. L. 2000. Geochemistry of the Archean Kam Group, Yellowknife Greenstone Belt, Slave Province, Canada. *Journal of Geology*, **108**, 181.

Cox, D. M., Frost, C. D. & Chamberlain, K. R. 2000. 2.01-Ga Kennedy dike swarm, southeastern Wyoming: Record of a rifted margin along the southern Wyoming province. *Rocky Mountain Geology*, **35**, 7–30, http://doi.org/10.2113/35.1.7

Crowley, P. D., Reiners, P. W., Reuter, J. M. & Kaye, G. D. 2002. Laramide exhumation of the Bighorn

Mountains, Wyoming: An apatite (U-Th)/He thermochronology study. *Geology*, **30**, 27–30, http://doi.org/10.1130/0091-7613(2002)030<0027:leotbm>2.0.co;2

Dahl, P. S., Holm, D. K., Gardner, E. T., Hubacher, F. A. & Foland, K. A. 1999. New constraints on the timing of Early Proterozoic tectonism in the Black Hills (South Dakota), with implications for docking of the Wyoming province with Laurentia. *Geological Society of America Bulletin*, **111**, 1335–1349.

Dahl, P. S., Hamilton, M. A., Wooden, J. L., Foland, K. A., Frei, R., McCombs, J. A. & Holm, D. K. 2006. 2480 Ma mafic magmatism in the northern Black Hills, South Dakota: a new link connecting the Wyoming and Superior cratons. *Canadian Journal of Earth Sciences*, **43**, 1579–1600.

Delaney, P. T. 1987. *Heat Transfer during Emplacement and Cooling of Mafic Dykes*. Geological Association of Canada, St John's, Newfoundland, Special Papers, **34**, 31–46.

Denson, N. M. & Pipiringos, G. N. 1974. *Geologic map & sections showing areal distribution of Tertiary rocks near the southeastern terminus of the Wind River Range, Fremont & Sweetwater counties, Wyoming*. USGS Miscellaneous Investigations Series Map **I-835**.

Ernst, R. & Bleeker, W. 2010. Large igneous provinces (LIPs), giant dyke swarms, and mantle plumes: significance for breakup events within Canada and adjacent regions from 2.5 Ga to the Present. *Canadian Journal of Earth Sciences*, **47**, 695–739.

Evans, D. A. D. & Halls, H. C. 2010. Restoring proterozoic deformation within the superior craton. *Precambrian Research*, **183**, 474–489.

Everitt, C. W. F. & Clegg, J. A. 1962. A field test of palaeomagnetic stability. *Geophysical Journal International*, **6**, 312–319, http://doi.org/10.1111/j.1365-246X.1962.tb00354.x

Fan, M. & Carrapa, B. 2014. Late Cretaceous-early Eocene Laramide uplift, exhumation and basin subsidence in Wyoming: crustal responses to flat slab subduction. *Tectonics*, **33**, 2012TC003221, http://doi.org/10.1002/2012TC003221

Foster, D. A., Mueller, P. A., Mogk, D. W., Wooden, J. L. & Vogl, J. J. 2006. Proterozoic evolution of the western margin of the Wyoming craton: implications for the tectonic and magmatic evolution of the northern Rocky Mountains. *Canadian Journal of Earth Sciences*, **43**, 1601–1619.

Frost, C. D. & Fanning, C. M. 2006. Archean geochronological framework of the Bighorn Mountains, Wyoming. *Canadian Journal of Earth Sciences*, **43**, 1399–1418.

Frost, C. D., Frost, B. R., Chamberlain, K. R. & Hulsebosch, T. P. 1998. The Late Archean history of the Wyoming province as recorded by granitic magmatism in the Wind River Range, Wyoming. *Precambrian Research*, **89**, 145–173.

Frost, C. D., Frost, B. R., Kirkwood, R. & Chamberlain, K. R. 2006*a*. The tonalite–trondhjemite–granodiorite (TTG) to granodiorite–granite (GG) transition in the late Archean plutonic rocks of the central Wyoming Province. *Canadian Journal of Earth Sciences*, **43**, 1419–1444.

Frost, C. D., Fruchey, B. L., Chamberlain, K. R. & Frost, B. R. 2006*b*. Archean crustal growth by lateral accretion of juvenile supracrustal belts in the south-central Wyoming Province. *Canadian Journal of Earth Sciences*, **43**, 1533–1555, http://doi.org/10.1139/e06-092

Gay, S. P. 2003. The 'Great Dike of Wyoming' and satellite bodies: a comparison to the Great Dyke of Rhodesia/Zimbabwe. *In*: Horn, M. S. (ed.) *2002 Field Conference 'Wyoming Basins' and 2003 Field Conference*. Wyoming Geological Association, Casper, WY, 101–111.

Grace, R. L. B., Chamberlain, K. R., Frost, B. R. & Frost, C. D. 2006. Tectonic histories of the Paleo- to Mesoarchean Sacawee block and Neoarchean Oregon Trail structural belt of the south-central Wyoming Province. *Canadian Journal of Earth Sciences*, **43**, 1445–1466.

Graff, P. 1979. A review of the stratigraphy and uranium potential of early Proterozoic (Precambrian X) metasediments in the Sierra Madre, Wyoming. *Rocky Mountain Geology*, **17**, 149–157.

Halgedahl, S. L. & Jarrard, R. D. 1995. Low-temperature behavior of single-domain through multi-domain magnetite. *Earth and Planetary Science Letters*, **130**, 127–139.

Halls, H. C. 1986. Paleomagnetism, structure, and longitudinal correlation of Middle Precambrian dykes from northwestern Ontario and Minnesota. *Canadian Journal of Earth Sciences*, **23**, 142–157, http://doi.org/10.1139/e86-018

Halls, H. C. 1991. The Matachewan dyke swarm, Canada: an early Proterozoic magnetic field reversal. *Earth and Planetary Science Letters*, **105**, 279–292, http://doi.org/10.1016/0012-821X(91)90137-7

Halls, H. C. & Davis, D. W. 2004. Paleomagnetism and U–Pb geochronology of the 2.17 Ga Biscotasing dyke swarm, Ontario, Canada: evidence for vertical-axis crustal rotation across the Kapuskasing Zone. *Canadian Journal of Earth Sciences*, **41**, 255–269.

Halls, H. C. & Zhang, B. 2003. Crustal uplift in the southern Superior Province, Canada, revealed by paleomagnetism. *Tectonophysics*, **362**, 123–136, http://doi.org/10.1016/S0040-1951(02)00634-0

Halls, H. C., Stott, G. M. & Davis, D. W. 2005. *Paleomagnetism, Geochronology and Geochemistry of Several Proterozoic Mafic Dike Swarms in Northwestern Ontario*. Ontario Geological Survey, Open File Report, **6171**.

Halls, H. C., Davis, D. W., Stott, G. M., Ernst, R. E. & Hamilton, M. A. 2008. The Paleoproterozoic Marathon Large Igneous Province: New evidence for a 2.1 Ga long-lived mantle plume event along the southern margin of the North American Superior Province. *Precambrian Research*, **162**, 327–353.

Hamilton, M. A. & Stott, G. M. 2008. The significance of new U/Pb baddeleyite ages from two Paleoproterozoic diabase dikes in Northern Ontario. Ontario Geological Survey, Open File Report, **6226**, 17-11–17-10.

Hamilton, M. A., Ryan, A. B., Emslie, R. F. & Ermanovics, I. F. 1998. Identification of Paleoproterozoic anorthositic and monzonitic rocks in the vicinity of the Mesoproterozoic Nain Plutonic Suite, Labrador:

U–Pb evidence. *Geological Survey of Canada, Current Research*, **1998-F**, 23–40.

Hamilton, M. A., Davis, D. W., Buchan, K. L. & Halls, H. C. 2002. *Precise U–Pb Dating of Reversely Magnetized Marathon Diabase Dykes and Implications for Emplacement of Giant Dyke Swarms along the Southern Margin of the Superior Province, Ontario*. Report **15**, Current Research 2002-F6 Radiogenic age and Isotopic Studies, Geological Survey of Canada.

Hark, J. S., Frei, R., Whitehouse, M. J. & Dahl, P. S. 2008. New evidence for 2.01 Ga rifting of the easternmost Wyoming craton (Black Hills, South Dakota): Implications for break-up of a supercraton (Superia). *Geological Society of America Abstracts with Programs*, **40**, 145.

Harlan, S. S., Geissman, J. W. & Premo, W. R. 2003. Paleomagnetism and geochronology of an Early Proterozoic quartz diorite in the southern wind river range, Wyoming, USA. *Tectonophysics*, **362**, 105–122.

Harms, T. A., Brady, J. B., Burger, H. R. & Cheney, J. T. 2004. *Advances in the Geology of the Tobacco Root Mountains, Montana, and their Implications for the History of the Northern Wyoming Province*. Geological Society of America, Boulder, CO, Special Papers, **377**, 227–243, http://doi.org/10.1130/0-8137-2377-9.227

Hausel, W. D. 1988. Geologic map of the Radium Springs Quadrangle including the Lewiston gold district, Fremont County, Wyoming. *Wyoming State Geological Survey Map Series*, **26**.

Hausel, W. D. 1991. *Economic geology of the South Pass Granite–Greenstone Belt, southern Wind River Range, Western Wyoming*. Geological Survey of Wyoming, Report of Investigations, **129**.

Heaman, L. M. 1997. Global mafic magmatism at 2.45 Ga; remnants of an ancient large igneous province? *Geology*, **25**, 299–302.

Heaman, L. M. & LeCheminant, A. N. 1993. Paragenesis and U–Pb systematics of baddeleyite (ZrO_2). *Chemical Geology*, **110**, 95–126, http://doi.org/10.1016/0009-2541(93)90249-I

Heimlich, R. A. & Armstrong, R. L. 1972. Variance of Precambrian K–Ar biotite dates, Bighorn Mountains, Wyoming. *Earth and Planetary Science Letters*, **14**, 75–78, http://doi.org/10.1016/0012-821X(72)90083-0

Heimlich, R. A., Nelson, G. C. & Gallagher, G. L. 1973. Metamorphosed mafic dikes from the southern Bighorn Mountains, Wyoming. *Geological Society of America Bulletin*, **84**, 1439–1450.

Hinrichs, E. N., Kent, B. H. & Pierce, F. W. 1990. *Bedrock geologic map and coal sections in the Buffal 30′ × 60′ Quadrangle, Johnson and Campbell counties, Wyoming*. USGS Miscellaneous Investigations Series I-1923-A.

Hoffman, P. F. 1988. United Plates of America, the birth of a craton: Early Proterozoic assembly and growth of Laurentia. *Annual Reviews in Earth and Planetary Science*, **16**, 543–603.

Hoffman, P. F. 1997. Tectonic genealogy of North America. *In*: Van der Pluijm, B. A. & Marshak, S. (eds) *Earth Structure: An Introduction to Structural Geology and Tectonics*. McGraw-Hill, New York, 459–464.

Hoppin, R. A., Palmquist, J. C. & Williams, L. O. 1965. Control by Precambrian basement structure on the location of the Tensleep-Beaver Creek fault, Bighorn Mountains, Wyoming. *The Journal of Geology*, **73**, 189–195, http://doi.org/10.2307/30066390

Houston, R. S. 1993. Late Archean and early Proterozoic geology of southeastern Wyoming. *Geology of Wyoming: Geological Survey of Wyoming Memoir*, **5**, 78–116.

Hoy, R. G. & Ridgway, K. D. 1997. Structural and sedimentological development of footwall growth synclines along an intraforeland uplift, east-central Bighorn Mountains, Wyoming. *Geological Society of America Bulletin*, **109**, 915–935, http://doi.org/10.1130/0016-7606(1997)109<0915:sasdof>2.3.co;2

Jones, C. H. 2002. User-driven integrated software lives: ‘Paleomag’ paleomagnetics analysis on the Macintosh. *Computers and Geosciences*, **28**, 1145–1151.

Kamber, B. S., Collerson, K. D., Moorbath, S. & Whitehouse, M. J. 2003. Inheritance of early Archaean Pb-isotope variability from long-lived Hadean protocrust. *Contributions to Mineralogy and Petrology*, **145**, 25–46, http://doi.org/10.1007/s00410-002-0429-7

Karlstrom, K. E., Flurkey, A. J. & Houston, R. S. 1983. Stratigraphy and depositional setting of the Proterozoic Snowy Pass Supergroup, southeastern Wyoming: record of an early Proterozoic Atlantic-type cratonic margin. *Geological Society of America Bulletin*, **94**, 1257–1274.

Keir, D., Pagli, C., Bastow, I. D. & Ayele, A. 2011. The magma-assisted removal of Arabia in Afar: evidence from dike injection in the Ethiopian rift captured using InSAR and seismicity. *Tectonics*, **30**, TC2008, http://doi.org/10.1029/2010TC002785

Kirschvink, J. L. 1980. The least-squares line and plane and the analysis of palaeomagnetic data. *Geophysical Journal International*, **62**, 699–718, http://doi.org/10.1111/j.1365-246X.1980.tb02601.x

Kirschvink, J. L., Kopp, R. E., Raub, T. D., Baumgartner, C. T. & Holt, J. W. 2008. Rapid, precise, and high-sensitivity acquisition of paleomagnetic and rock-magnetic data: development of a low-noise automatic sample changing system for superconducting rock magnetometers. *Geochemistry, Geophysics, Geosystems*, **9**, Q05Y01, http://doi.org/10.1029/2007gc001856

Krogh, T. E. 1973. A low-contamination method for hydrothermal decomposition of zircon and extraction of U and Pb for isotopic age determinations. *Geochimica et Cosmochimica Acta*, **37**, 485–494, http://doi.org/10.1016/0016-7037(73)90213-5

Love, J. D. & Christiansen, A. C. 1985. *Geologic map of Wyoming*. US Geological Survey, Reston, VA.

Luais, B. & Hawkesworth, C. J. 2002. Pb isotope variations in Archaean time and possible links to the sources of certain Mesozoic–Recent basalts. *In*: Fowler, C. M. R., Ebinger, C. J. & Hawkesworth, C. J. (eds) *The Early Earth: Physical, Chemical and Biological Development*. Geological Society, London, Special Publications, **199**, 105–124, http://doi.org/10.1144/gsl.sp.2002.199.01.06

Ludwig, K. R. 1988. *PBDAT for MS-DOS, a computer program for IBM-PC compatibles for processing raw Pb–U–Th isotope data, version 1.24*. US Geological Survey, Open-File Report **88-542**.

Ludwig, K. R. 1991. *ISOPLOT for MS-DOS, a plotting and regression program for radiogenic-isotope data, for IBM-PC compatible computers, version 2.75*. US Geological Survey, Open-File Report **91-445**.

Maurice, C., David, J., O'Neil, J. & Francis, D. 2009. Age and tectonic implications of Paleoproterozoic mafic dyke swarms for the origin of 2.2 Ga enriched lithosphere beneath the Ungava Peninsula, Canada. *Precambrian Research*, **174**, 163–180.

Mitchell, R. N., Hoffman, P. F. & Evans, D. A. D. 2010. Coronation loop resurrected: Oscillatory apparent polar wander of Orosirian (2.05–1.8 Ga) paleomagnetic poles from Slave craton. *Precambrian Research*, **179**, 121–134.

Mogk, D. W., Mueller, P. A. & Wooden, J. L. 1988. Archean Tectonics of the North Snowy Block, Beartooth Mountains, Montana. *The Journal of Geology*, **96**, 125–141.

Mogk, D. W., Mueller, P. A. & Wooden, J. L. 1992. The nature of Archean terrane boundaries: an example from the northern Wyoming Province. *Precambrian Research*, **55**, 155–168, http://doi.org/10.1016/0301-9268(92)90020-o

Mueller, P. A. & Frost, C. D. 2006. The Wyoming Province: a distinctive Archean craton in Laurentian North America. *Canadian Journal of Earth Sciences*, **43**, 1391–1397, http://doi.org/10.1139/e06-075

Mueller, P. A., Wooden, J. L., Mogk, D. W., Nutman, A. P. & Williams, I. S. 1996. Extended history of a 3.5 Ga trondhjemitic gneiss, Wyoming Province, USA: evidence from U–Pb systematics in zircon. *Precambrian Research*, **78**, 41–52, http://doi.org/10.1016/0301-9268(95)00067-4

Mueller, P. A., Heatherington, A. L., Kelly, D. M., Wooden, J. L. & Mogk, D. W. 2002. Paleoproterozoic crust within the Great Falls tectonic zone: implications for the assembly of southern Laurentia. *Geology*, **30**, 127–130, http://doi.org/10.1130/0091-7613(2002)030<0127:pcwtgf>2.0.co;2

Mueller, P. A., Burger, H. R., Wooden, J. L., Heatherington, A. L., Mogk, D. W. & D'Arcy, K. 2004. *Age and Evolution of the Precambrian Crust of the Tobacco Root Mountains, Montana*. Geological Society of America, Boulder, CO, Special Papers, **377**, 181–202, http://doi.org/10.1130/0-8137-2377-9.181

Mueller, P. A. & Burger, H. R. *et al.* 2005. Paleoproterozoic metamorphism in the Northern Wyoming Province: implications for the assembly of Laurentia. *The Journal of Geology*, **113**, 169–179, http://doi.org/10.1086/427667

Muxworthy, A. R. & Williams, W. 2006. Low-temperature cooling behavior of single-domain magnetite: forcing of the crystallographic axes and interactions. *Journal of Geophysical Research: Solid Earth*, **111**, B07103, http://doi.org/10.1029/2006JB004298

Noble, S. R. & Lightfoot, P. C. 1992. U–Pb baddeleyite ages of the Kerns and Triangle Mountain intrusions, Nipissing Diabase, Ontario. *Canadian Journal of Earth Sciences*, **29**, 1424–1429, http://doi.org/10.1139/e92-114

Osterwald, F. W. 1978. Structure and petrology of the northern Big Horn Mountains, Wyoming. *The Geological Survey of Wyoming, Bulletin*, **48**, 1–47.

Parrish, R. R., Roddick, J. C., Loveridge, W. D. & Sullivan, R. D. 1987. *Uranium–lead analytical techniques at the Geochronology Laboratory, Geological Survey of Canada*. Radiogenic age and isotopic studies: Report 1 Geological Survey of Canada, Paper **87-2**.

Peng, P., Zhai, M., Zhang, H. & Guo, J. 2005. Geochronological constraints on the Paleoproterozoic evolution of the North China Craton: SHRIMP Zircon ages of different types of Mafic Dikes. *International Geology Review*, **47**, 492–508, http://doi.org/10.2747/0020-6814.47.5.492

Premo, W. R. & Van Schmus, W. R. 1989. *Zircon Geochronology of Precambrian Rocks in Southeastern Wyoming and Northern Colorado*. Geological Society of America, Boulder, CO, Special Papers, **235**, 13–32, http://doi.org/10.1130/SPE235-p13

Redden, J. A., Peterman, Z. E., Zartman, R. E. & DeWitt, E. 1990. *U–Th–Pb geochronology and preliminary interpretation of Precambrian tectonic events in the Black Hills, South Dakota*. The Trans-Hudson orogen: Geological Association of Canada Special Paper, **37**, 229–251.

Rioux, M., Bowring, S., Dudás, F. & Hanson, R. 2010. Characterizing the U–Pb systematics of baddeleyite through chemical abrasion: application of multi-step digestion methods to baddeleyite geochronology. *Contributions to Mineralogy and Petrology*, **160**, 777–801, http://doi.org/10.1007/s00410-010-0507-1

Roberts, A. P. 2008. Geomagnetic excursions: knowns and unknowns. *Geophysical Research Letters*, **35**, L17307, http://doi.org/10.1029/2008GL034719

Rogers, J. J. W. & Santosh, M. 2002. Configuration of Columbia, a Mesoproterozoic supercontinent. *Gondwana Research*, **5**, 5–22.

Rohon, M. L., Vialette, Y., Clark, T., Roger, G., Ohnenstetter, D. & Vidal, P. 1993. Aphebian mafic–ultramafic magmatism in the Labrador Trough (New Quebec): its age and the nature of its mantle source. *Canadian Journal of Earth Sciences*, **30**, 1582–1593, http://doi.org/10.1139/e93-136

Roscoe, S. M. 1969. *Huronian rocks and uraniferous conglomerates in the Canadian shield*. Geological Survey of Canada, Ottawa, Papers, **68–40**, 205, http://doi.org/10.4095/102290

Roscoe, S. M. & Card, K. D. 1993. The reappearance of the Huronian in Wyoming: rifting and drifting of ancient continents. *Canadian Journal of Earth Sciences*, **30**, 2475–2480.

Schwarz, E. J., Buchan, K. L. & Cazavant, A. 1985. Post-Aphebian uplift deduced from remanent magnetization, Yellowknife area of Slave Province. *Canadian Journal of Earth Sciences*, **22**, 1793–1802, http://doi.org/10.1139/e85-190

Selkin, P. A., Gee, J. S., Meurer, W. P. & Hemming, S. R. 2008. Paleointensity record from the 2.7 Ga Stillwater Complex, Montana. *Geochemistry Geophysics Geosystems*, **9**, Q12023.

Sigurdsson, H. 1987. Dyke injection in Iceland: a review. *In*: Halls, H. C. & Fahrig, W. H. (eds) *Mafic Dyke Swarms*. Geological Association of Canada, St John's, Newfoundland, Special Papers, **34**, 55–64.

Sims, P. K., Finn, C. A. & Rystrom, V. L. 2001. *Preliminary Precambrian basement map showing geologic – geophysical domains, Wyoming*. US Geological Survey, Open-File Report **01-199**, 9.

Smithson, S. B., Brewer, J. A., Kaufman, S., Oliver, J. E. & Hurich, C. A. 1979. Structure of the Laramide Wind River uplift, Wyoming, from COCORP deep reflection data and from gravity data. *Journal of Geophysical Research*, **84**, 5955–5972, http://doi.org/10.1029/JB084iB11p05955

Smithson, S. B., Brewer, J. A., Kaufman, S., Oliver, J. E. & Zawislak, R. L. 1980. Complex Archean lower crustal structure revealed by COCORP crustal reflection profiling in the wind river range, Wyoming. *Earth and Planetary Science Letters*, **46**, 295–305.

Snyder, G. L., Hughes, D. J., Hall, R. P. & Ludwig, K. R. 1989. *Distribution of Precambrian mafic intrusions penetrating some Archean rocks of western North America*. US Geological Survey, Open-File Report **89–125**, 36.

Söderlund, U. & Johansson, L. 2002. A simple way to extract baddeleyite (ZrO2). *Geochemistry, Geophysics, Geosystems*, **3**, 1–7, http://doi.org/10.1029/2001GC000212

Stacey, J. S. & Kramers, J. D. 1975. Approximation of terrestrial lead isotope evolution by a two-stage model. *Earth and Planetary Science Letters*, **26**, 207–221, http://doi.org/10.1016/0012-821X(75)90088-6

Steiger, R. H. & Jäger, E. 1977. Subcommission on geochronology: convention on the use of decay constants in geo- and cosmochronology. *Earth and Planetary Science Letters*, **36**, 359–362, http://doi.org/10.1016/0012-821X(77)90060-7

St-Onge, M. R., Searle, M. P. & Wodicka, N. 2006. Trans-Hudson Orogen of North America and Himalaya–Karakoram–Tibetan Orogen of Asia: structural and thermal characteristics of the lower and upper plates. *Tectonics*, **25**, TC4006, http://doi.org/10.1029/2005tc001907

Stueber, A. M., Heimlich, R. A. & Ikramuddin, M. 1976. Rb–Sr ages of Precambrian mafic dikes, Bighorn Mountains, Wyoming. *Geological Society of America Bulletin*, **87**, 909–914, http://doi.org/10.1130/0016-7606(1976)87<909:raopmd>2.0.co;2

Sun, S.-s. & McDonough, W. F. 1989. Chemical and isotopic systematics of oceanic basalts: implications for mantle composition and processes. *In*: Saunders, A. D. & Norry, A. J. (eds) *Magmatism in Ocean Basins*. Geological Society, London, Special Publications, **42**, 313–345, http://doi.org/10.1144/gsl.sp.1989.042.01.19

Thaden, R. E. 1980. *Geologic map of the De Pass quadrangle, Fremont and Hot Springs Counties, Wyoming*. US Geological Survey Geological Quadrangle Map **1526**.

Tsai, V. C. & Stevenson, D. J. 2007. Theoretical constraints on true polar wander. *Journal of Geophysical Research: Solid Earth*, **112**, B05415, http://doi.org/10.1029/2005JB003923

Vuollo, J. & Huhma, H. 2005. Paleoproterozoic mafic dikes in NE Finland. *Developments in Precambrian Geology*, **14**, 195–236.

Wall, E. N. 2004. *Petrologic, geochemical, and isotopic constraints on the origin of 2.6 Ga post-tectonic granitoids of the central Wyoming Province*. Unpublished MS thesis, University of Wyoming.

Weil, A. B., Yonkee, A., Statman-Weil, Z. & Wicks, D. 2009. Determining the 3-D kinematic History of the Wyoming Laramide Foreland: Preliminary Results from a Paleomagnetic Investigation of the Triassis Chugwater Group. *Geological Society of America Abstracts with Programs*, Portland, OR, 692.

Williams, H., Hoffman, P. F., Lewry, J. F., Monger, J. W. H. & Rivers, T. 1991. Anatomy of North America: thematic geologic portrayals of the continent. *Tectonophysics*, **187**, 117–134.

Young, G. M. 1970. An extensive early proterozoic glaciation in North America? *Palaeogeography, Palaeoclimatology, Palaeoecology*, **7**, 85–101, http://doi.org/10.1016/0031-0182(70)90070-2

Young, G. M., Long, D. G. F., Fedo, C. M. & Nesbitt, H. W. 2001. Paleoproterozoic Huronian basin: product of a Wilson cycle punctuated by glaciations and a meteorite impact. *Sedimentary Geology*, **141–142**, 233–254.

Zhao, G., Cawood, P. A., Wilde, S. A. & Sun, M. 2002. Review of global 2.1–1.8 Ga orogens: implications for a pre-Rodinia supercontinent. *Earth-Science Reviews*, **59**, 125–162.